

STUDY OF THE GROWTH AND DISSOLUTION

OF COPPER WHISKERS

STUDY OF THE GROWTH AND DISSOLUTION
OF COPPER WHISKERS

By

Eric James Hayes A.R.C.S.T.

A Thesis

Submitted to the Faculty of Graduate Studies
in Partial Fulfillment of the Requirements
for the Degree
Master of Science

McMaster University

(October) 1965

ACKNOWLEDGMENTS

The author wishes to acknowledge the help of his supervisor, Dr. M. B. Ives, for his numerous suggestions and interest in the research problem.

Thanks are also due to Dr. W. W. Smeltzer and Mr. T. R. Ramachandran for guidance on electro-chemical aspects of the problem, and to Dr. Feidler for performing the activation analysis.

The work was performed with the support of the U. S. Office of Naval Research and the National Research Council of Canada.

SUMMARY

Copper whiskers were grown by the chemical reduction of cuprous iodide by hydrogen using Brenner's technique.⁴³ The whiskers were dissolved electrolytically in acidified copper sulphate at a current density of 1.5 micro-amps per square cm. The etched cross-sectional profiles were used to determine the dissolution rate of major orientations.

TABLE OF CONTENTS

	<u>Page</u>
CHAPTER I. INTRODUCTION	1
<u>Introduction</u>	1
<u>Surface and Surface Energy</u>	2
<u>Surface Diffusion</u>	5
<u>Structure and Morphologies of Whiskers</u>	7
<u>Review of Previous Work</u>	9
CHAPTER II. THEORY OF WHISKER GROWTH	13
<u>Introduction</u>	13
<u>Mechanistic Approach to Whisker Growth</u>	14
<u>Recent Experimental Evidence on</u> <u>Filamentary Growths</u>	16
<u>Vapour-Liquid-Solid Theory (V-L-S)</u>	17
CHAPTER III. THEORY OF DISSOLUTION	20
<u>Introduction</u>	20
<u>Mechanistic Theory (B. C. F.)</u>	20
<u>Kinematic Theory of Crystal Dissolution</u>	23
<u>Kinematic Theory Applied to Macroscopic</u> <u>Symmetry Sections</u>	29
<u>Criticism of the Theory</u>	31
<u>Comparison with Experiment</u>	33
CHAPTER IV. FILAMENTARY GROWTH	35
<u>Experimental Procedure</u>	35
<u>Variables in the Growth Process</u>	36
<u>Handling of the Whiskers</u>	39
<u>Analysis</u>	39

	<u>Page</u>
CHAPTER V. DISSOLUTION EXPERIMENTS	40
<u>Introduction</u>	40
<u>The Apparatus</u>	42
<u>Surface Examination</u>	43
<u>Cross Sectional Examination</u>	45
<u>Correlation of Cross Sectional Shapes</u>	47
CHAPTER VI. RESULTS	50
<u>Growth</u>	50
<u>Dissolution</u>	52
<u>Cross Sectional Results</u>	53
CHAPTER VII. DISCUSSION	55
<u>Introduction</u>	55
<u>Discussion of Growth Experiments</u>	56
<u>Growth Mechanism</u>	58
<u>Growth Morphologies</u>	58
<u>Dissolution</u>	59
CHAPTER VIII. CONCLUSIONS	63
BIBLIOGRAPHY	64
APPENDIX I	69
APPENDIX II	70

CHAPTER I

INTRODUCTION

Introduction

If a metal is cleaved on close-packed planes then, in general, the exposed surfaces will not be completely flat on the atomic scale, but consist of terraces separated at random intervals by ledges. The ledges themselves are not uniform but contain deviations from perfect periodicity resulting in an increase in surface entropy and corresponding decrease in energy.

The process of dissolution takes place by the atoms breaking the bonds at these places of perturbation, called kinked sites, causing the ledge to diminish in length. The subsequent motion and interaction of the ledges results in the metal surface being dissolved. The resultant structure of the surface may appear pitted, polished or faceted depending on how the ledge motion is initiated, and in what manner and with what velocity it proceeds.

The geometrical symmetry of these facets or pits is a function of, among other things, the crystallographic orientation of the exposed face of the material. Current theories of dissolution

(to be described in Chapter IV) incorporate this orientation dependence of dissolution.

The aim of this research was to detect reactivity as a function of crystallographic orientation for perfect metal whiskers. It would then be possible to compare the results with those obtained from the dissolution of bulk copper by Young and Eulett.¹⁴

The growth of whiskers was also studied since the growth mechanism had strong bearing on dissolution topography.

Surface and Surface Energy

The first approach to a description of a surface was sought from thermodynamics by Gibbs.¹ Gibbs introduced a definition of surface free energy, permitting the concept of surface tension to be extended to the solid state. He went further to introduce anisotropic surface free energy from which he postulated non-spherical equilibrium shapes, which, from a thermodynamic argument, define a shape having a minimal total surface free energy.

The anisotropy of surface free energy as a function of orientation has been plotted as a polar diagram by Wulff,² and from this diagram surfaces may be categorized. This diagram (Figure 8, Chapter IV) will be described more fully later.

Frank³ and Cabrera⁴ have categorized surfaces as:

(1) Singular surfaces, corresponding to grooved minima in the Wulff Plot of interfacial free energy as a function of

orientation (usually low-index planes).

(2) Vicinal surfaces, with orientations near those of a singular surface and formed of low index facets separated by monomolecular ledges or steps.

(3) Non Singular or Diffuse surfaces, whose interfacial free energy is roughly independent of orientation.

Kossel,⁵ and Burton, Cabrera and Frank⁶ incorporated the fundamental ideas of Gibbs to describe the currently accepted geometric model for vicinal surfaces as shown schematically in Figure 1.

Basically a vicinal surface is composed of low-index facets separated by monatomic ledges lying in low-index directions except for random monatomic perturbations, i.e. kinks.* Therefore, a macroscopic surface having a mean orientation deviating by a small angle (θ) from a singular surface is actually composed of an array of steps on a microscopic scale.

A number of steps proportional to θ will end on the surface, each increasing the energy of the surface. This increase in surface energy results simply from the greater amount of surface present. Hence, it follows that for well separated steps there will be an increase in the surface energy (γ) proportional to the length of the step introduced. Similarly, each step will increase the

* Kinks are illustrated schematically in Figure 1(c).

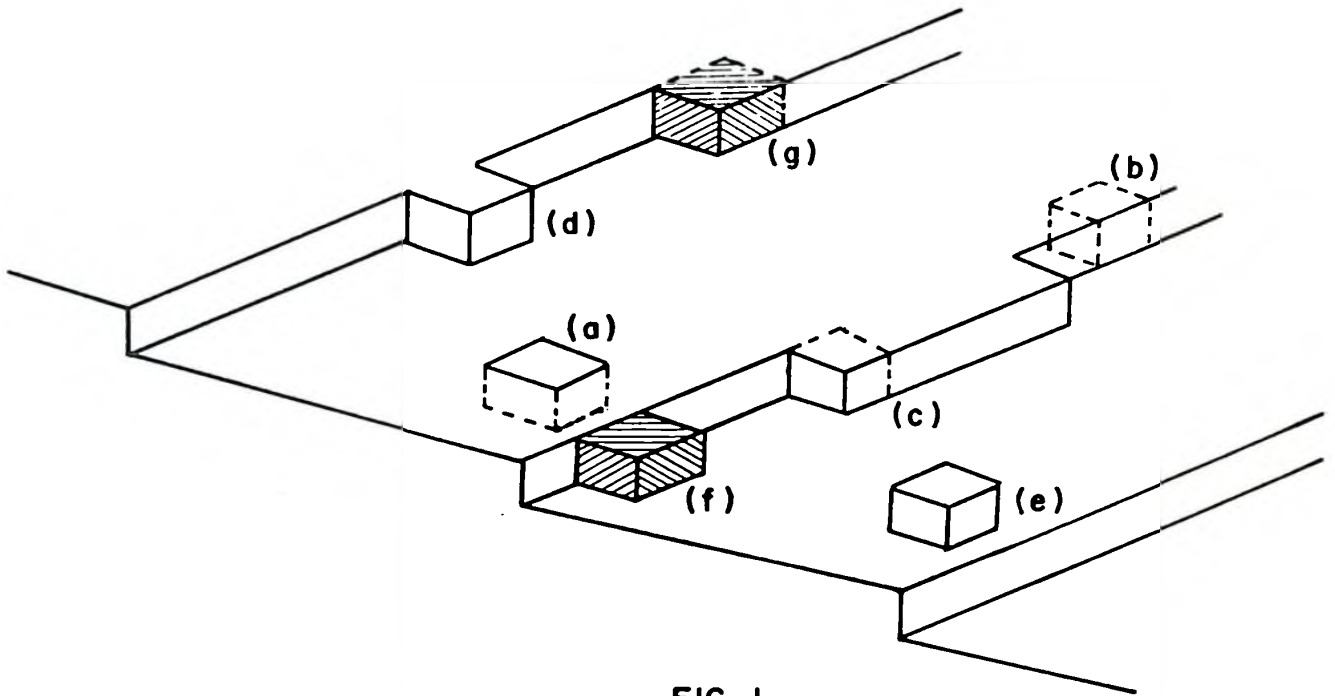


FIG. 1

MICROSCOPIC MODEL OF A SURFACE

- (a) Atom in surface
- (b) Atom in ledge
- (c) Atom at kink
- (d) Atom in ledge
- (e) Atom on surface
- (g) Poisoned kink
- (f) Impurity atom at ledge

entropy of the surface. The energy and the entropy combine to give a change in the free energy of the surface that is proportional to Θ .

An important result of this model is derived in Appendix I and may be summarized by the following equation:

$$\gamma = \gamma_0 (\cos \Theta + \sin \Theta) \quad (1)$$

where γ_0 is the energy per unit area of a singular surface.

The conclusion from the above discussion is that γ versus Θ will have discontinuities in its slope, and that the magnitude of the discontinuity is proportional to the free energy increase per step added. This γ versus Θ plot was first derived by Wulff² and is termed the Wulff-Plot.

The Wulff plot is important since the equilibrium shape of a crystal may be derived by applying a construction to the polar diagram. This construction -- the Wulff construction -- states:⁷ "Given the polar diagram of surface free energy, composed of surfaces whose radii are $\bar{n}\gamma$, the equilibrium shape is to be found as the inner envelope of planes normal to these radii at their distal points."

The Wulff Plot and construction for a two fold axis of symmetry are shown as the two outside figures in Figure 8.

Surface Diffusion

The basis of growth from the vapour may be summarized as (1) condensation of vapour atoms onto the surface, (2) diffusion of the adsorbed atoms to a ledge and (3) diffusion along a ledge to a kink. Conversely, the fundamentals of the dissolution process may be regarded as (1) diffusion from a kink to a ledge, (2) diffusion from a ledge to a surface resulting in the movement of trains of ledges across the surface. As has been shown by Hirth and Pound,⁸ surface diffusion is of great importance when considering growth or dissolution so it is relevant to briefly consider the topic.

It is well known that a crystal lattice in equilibrium contains a certain concentration of vacancies (n_v) which depend exponentially on temperature according to the relation

$$n_v = n_0 \exp - \frac{W_v}{kT} \quad (2)$$

where n_0 is the number of lattice points and W_v is the energy to form a vacancy.

On exactly the same statistical mechanical basis it has been shown that singular surfaces will develop surface vacancies of concentration $n_v^{(s)}$ and surface adsorbed atoms of concentration $n^{(s)}$. Both surface concentrations are analogous to the above formula, i.e.

$$n_v^{(s)} = n_0^{(s)} \exp - \frac{W_v^{(s)}}{kT} \quad (3)$$

$$n^{(s)} = n_0^{(s)} \exp - \frac{W^{(s)}}{kT} \quad (4)$$

where $n_0^{(s)}$ is the number of surface lattice sites (approximately 10^{15} per cm^2).

Qualitative evaluations of the above equations⁹ reveal that the proportion of point defects on a surface is substantially higher than in the bulk. This is an important fact since it is point defects which control, at least partially, any transport process. Lattice fluctuations may cause a surface adsorbed atom to either jump to a neighbouring site on the surface or leave the surface. The frequency with which a point defect jumps on the crystal surface determines its surface diffusion coefficient $D^{(s)}$, which can be written as

$$D_v^{(s)} = a^2 \gamma \exp - \frac{U_v^{(s)}}{kT} \quad (5)$$

$$D^{(s)} = a^2 \gamma \exp - \frac{U^{(s)}}{kT} \quad (6)$$

where $U_v^{(s)}$ and $U^{(s)}$ are activation energies between neighbouring positions a distance "a" apart.

Since $U_v^{(s)} > U^{(s)}$ then $D^{(s)} > D_v^{(s)}$, this means that the mobility of adsorbed atoms is greater than the mobility of surface vacancies.

Besides the concentration ($n^{(s)}$) and the mobility (D^s) of the surface adsorbed atoms there is a third important parameter in surface diffusion, namely the lifetime of the atom in a state (τ_s). The mean lifetime of the adsorbed atom, i.e. the time between jumps, is given by,

$$\frac{1}{\tau_s} = \nu \exp - \frac{W_s'}{kT} \quad (7)$$

where W_s' is the energy required for an adatom to leave the surface and enter the solution.

Mobility, lifetime and mean displacement of an adsorbed atom (λ_s) are connected via Einstein's equation for random walk, viz,

$$\lambda_s = (D^s \tau_s)^{\frac{1}{2}} \quad (8)$$

Substituting equations (6) and (7) into (8) gives

$$\lambda_s = a \exp \left(\frac{W_s' - U^s}{2kT} \right) \quad (9)$$

The mean displacement of an adatom (λ_s) plays a very important role in crystal growth from the vapour (Chapter II) and in the mechanistic theory of dissolution (Chapter IV).

Structure and Morphologies of Whiskers

It has been suggested¹⁰ that the unusual properties of whiskers are associated with high three-dimensional perfection

i.e. the absence of dislocations or by the presence of insufficient number to produce multiplication. Small size itself results in a smaller probability of encountering defects; for example if dislocations are uniformly distributed in the crystal with a density of 10^6 dislocations per cm^2 they will be ten microns apart. A whisker with a diameter less than ten microns might therefore contain no dislocations. If this conclusion is correct then small crystals produced by etching down large crystals should have the same properties as whiskers, but this has been disproven experimentally.¹¹ Therefore, whiskers are different from bulk material because of certain peculiarities in their growth.

During the nucleation of the whisker under equilibrium conditions, the shape adopted by the nucleus must obey the dictates of thermodynamics, i.e. the "equilibrium shape" will possess the minimum total surface free energy and can be deduced from the Wulff Plot -- once the direction of growth is known (see for example Figure 8). The deduction of the "equilibrium shape" can only be performed accurately if growth occurs under strictly equilibrium conditions. The influence of kinetic control will affect the nucleus shape and so alter the equilibrium shape.

From crystallographic¹² and thermodynamic considerations, an "equilibrium shape" for a F. C. C. metal with a $\langle 111 \rangle$ growth axis should possess six sides. A priori, a $\langle 001 \rangle$ growth axis should

reflect a four-fold symmetry. Diagrams showing the geometry of these common types of whisker orientations are given in Figure 2.

That the filamentary growths do actually grow in this manner can be seen with reference to Figure 18.

Review of Previous Work

To the knowledge of the author, no previous work on the electro-chemical dissolution of copper whiskers has ever been performed. Recently, however, workers at Oak Ridge National Laboratories have completed work¹³ on the dissolution of copper single crystal needles.

Extensive work has been reported on the chemical reactivity of single crystalline copper surfaces, and in this connection the work of Young¹⁴ is outstanding.

Studies of the thermal etching of copper crystals in vacuum have been reported by several workers.¹⁵ It has been found that the number of pits formed was a function of the temperature of etching, the purity of the crystal and the crystal orientation. Further, the arrangement of pits did not correspond to that formed by dislocation etchants on similar crystals. Thus, it was concluded that at least there was not a one-to-one correspondence between thermal etch pits and dislocations. The thermal etching of copper crystals results in the formation of pits, ledges and facets. As

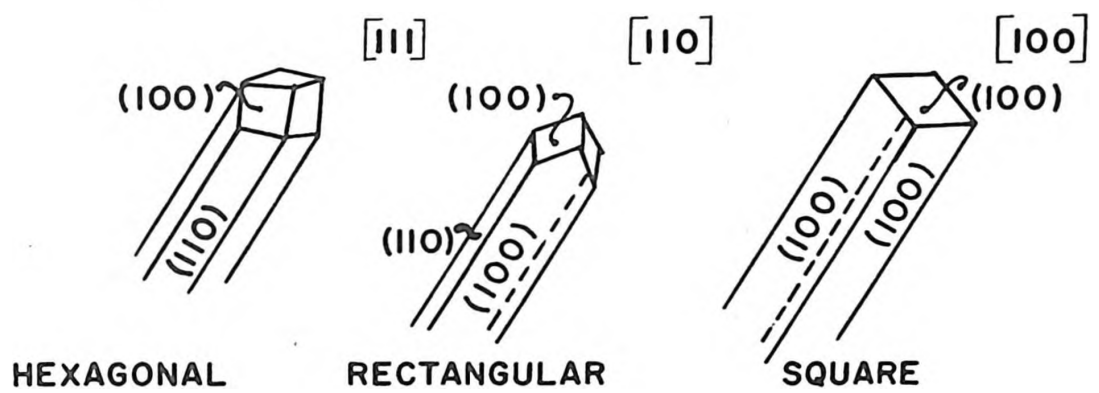


FIG. 2

GROWTH SHAPES AND MOST PROBABLE CRYSTALLOGRAPHIC ORIENTATIONS
FOR VARIOUS WHISKER GROWTH ZONES

yet, there is not complete agreement as to the cause of ledges observed after thermal etching. For example, Stosel¹⁶ has suggested that the ledges may be formed on cooling because of stresses arising from dissolved oxygen. It appears that, while thermal etching should be a good technique for studying the role of dislocations in the nucleation of steps, experimental conditions are very difficult.

Jenkins¹⁷ carried out a series of experiments which serve to demonstrate conditions under which dislocations play a significant role in the dissolution mechanism. In studies of the dissolution of several crystal faces of copper in air-saturated solutions of ethylenediamine, the rate of reaction was found to be controlled by the rate of diffusion of the dissolved oxygen to the metal surface. Therefore, the rate of dissolution was the same on all faces. However, facets that were characteristic of the particular crystal face were formed by the process.

The electrolytic dissolution of copper at low current densities in de-aerated solutions of acidified copper sulphate solutions have been performed by Bertocci¹⁸ and Jenkins.¹⁹ From this work it was found that at very low current densities (about two micro-amps per sq. cm.) dissolution occurred from steps present on the surface.

Etchants that form pits at dislocations on the close packed planes of copper have been developed by Young¹⁴ and Lovell and

Wernick,²⁰ Where the etch pit is formed at a clean dislocation i.e. no impurity atmosphere, the energy for the nucleation of the pit consists of the core and strain energies associated with the dislocation. Since the extra energy available for the nucleation of steps must be associated with the atoms involved in the nucleation process, the strain energy for only those atoms shall be considered. The strain energy in a cylinder around a dislocation 100 \AA in radius is comparable with the core energy of the dislocation. Although a good estimate of the core energy of the different types of dislocations is difficult, there is a difference in the energy available at edge and screw dislocations. This has been substantiated by Livingston,²¹ who observed that edge dislocations produce deeper pits than screw dislocations intersecting the surface.

Young¹⁴ has performed informative experiments on the electrolytic dissolution of copper, where he obtains a photomicrographic record of individual pit growth. From these photographs it was possible to obtain detailed information on the change in slope of the sides of the pit with depth into the pit. This is of particular interest in connection with current dissolution theory (see Chapter IV).

Since nucleation of steps proceeds at a greater rate at a dislocation than elsewhere on the surface, a series of ledges emanates from this source and a pit is formed. The edge of the

pit is defined by the leading ledge and therefore the rate of growth of the pit is determined by the ledge velocity. By judicious selection of experimental parameters it is now possible to not only control the ledge velocity, but change the mechanics of dissolution in a predicted manner. This is a major experimental achievement and will be discussed more fully in the chapter on dissolution theory.

Although no work has been performed on the fundamental aspects of dissolution of copper whiskers, some work has been completed on the corrosion of iron whiskers.^{22,23} Shemanski et al²² have shown that, for iron whiskers, at low undersaturations, the dissolution rate is a linear function of the ferrous ion in solution. At higher undersaturations the dissolution rate was found to be dependent upon the logarithm of the undersaturation ratios.

In both cases the dissolution rate was found to depend on the logarithm of the interfacial free energy, which is in accordance with the mechanistic model of a surface (Chapter III).

CHAPTER II

THEORY OF WHISKER GROWTH

Introduction

There are four general methods of producing filamentary single crystals ("whiskers"):

- (1) Electrodeposition,
- (2) Growth from the bulk solid phase,
- (3) Deposition from the solution,
- (4) Deposition from the vapour.

Each of these methods differ in experimental procedure and in their mechanism of growth. Since the copper whiskers of this study were grown from the vapour, the attention of this chapter is confined to the fourth method.

The classical ideas regarding the mechanism of crystal growth from the vapour were formulated by Gibbs¹ and developed by Kossel.⁵ According to the classical theory, the close-packed face of a growing crystal advances at a rate that is proportional to the frequency with which the nuclei of new atomic layers are created. The probability of nucleation, and therefore the growth rate of a face, is negligibly small until supersaturation reaches

the order of at least ten percent. By experiment, however, it can be shown that crystals grow at supersaturations even less than one percent.

This contradiction between theory and experiment was accounted for in 1949 by Frank²⁴ who pointed out that a surface intersected by a screw dislocation acquires a step, equal in height to the component of the Burgers Vector of the dislocation normal to the surface. Growth at dislocations can therefore proceed even under low supersaturations, so that growth rate is unlimited by nucleation rate.

Mechanistic Approach to Whisker Growth

Using the concept of the axial screw dislocation, the theory of whisker growth from the vapour phase has been evolved by Sears,²⁵ Gomer,²⁶ and Parker and Hardy.²⁷

The mass rate of impingement, \dot{W} , of atoms on the whisker end is given by the kinetic theory of gases as,

$$\dot{W} = \pi r^2 \times P \times \left(\frac{m}{2\pi kT}\right)^{\frac{1}{2}} \quad (10)$$

where r is the crystal radius, P is the vapour pressure, m is the atomic mass. Assuming that every atom which strikes the whisker end is incorporated into the metallic lattice then,

$$\dot{W} = \pi r^2 \times l \times \rho \quad (11)$$

where \dot{i} is the rate of increase in length per second; ρ is the density. From (10) and (11),

$$\dot{i} = \frac{\rho}{\rho} \left(\frac{m}{2\pi RT} \right)^{\frac{1}{2}} \quad (12)$$

For the specific case of copper whiskers this growth rate is

$$\dot{i} = 3 \times 10^{-6} \text{ cm/sec}$$

In this laboratory, however, a boat of copper whiskers averaging about 1 cm in length, grew in a period of one hour. Hence by experiment the average growth rate \dot{i} is,

$$\dot{i} = 3 \times 10^{-4} \text{ cm/sec}$$

The calculated growth rate is based on the hypothesis that only atoms striking the advancing whisker end contribute to axial growth. This discrepancy demonstrates that atoms striking elsewhere on the crystal surface are contributing to axial growth.

It was introduced in Chapter I that an atom adsorbed on a surface migrates a certain distance (the mean diffusion distance λ) during a certain time (the lifetime τ) before evaporation. Thus, atoms impinge on the sides of the crystal, are adsorbed and migrate a distance $\leq \lambda$ to the advancing tip, where they are incorporated into the crystal lattice.

The calculation of growth rate thus becomes a diffusion problem.

Dittmar and Neumann²⁸ have shown, by setting up a steady state surface diffusion equation with appropriate boundary conditions, that the whisker growth rate is given by,

$$\dot{i} = (N - N_0) \left(\frac{\lambda}{r}\right) \left(\frac{2m}{\rho}\right) \text{tanh} \left(\frac{l}{r}\right) \quad (13)$$

where N is the actual vapour flux; N_0 is the equilibrium vapour flux,

At the initial stages of whisker growth $\lambda > 1$, hence

$$\dot{i} = (N - N_0) \left(\frac{2m}{\rho r}\right) \times 1 \quad (14)$$

so giving an exponential mode of growth.

As λ becomes greater than 1 then

$$\dot{i} = (N - N_0) \left(\frac{2m}{\rho r}\right) \times \lambda \quad (15)$$

giving a linear growth law.

Parker and Hardy²⁷ have taken photographs of potassium and mercury whiskers growing and have verified exponential and linear stages of growth.

Recent Experimental Evidence on Filamentary Growths

Although the theory of whisker growth postulates the presence of an axial screw dislocation, the detection of such an imperfection by direct observation has not always yielded a positive result. Electron microscope studies of filamentary crystals of copper oxide²⁹

and aluminum nitride³⁰ have failed to reveal an axial dislocation. Indeed, Webb³¹ and co-workers examined whiskers of nine different metals grown from the vapour and found unequivocal evidence for a single axial dislocation in only one -- palladium.

In a boat of silicon crystals grown from the vapour by chemical reduction, filamentary crystals containing axial dislocations have been found growing beside similar crystals showing no evidence of dislocations having been present. The possibility that the axial dislocation slipped out of the whisker has been considered by Hirth⁵⁸ and found to be possible only for whiskers less than five microns. In this particular study of silicon whiskers, the crystals were greater than ten microns diameter so the explanation of the dislocation slipping is not feasible.

Since the whiskers with and without axial dislocations were grown under the same physico-chemical conditions, it can only be concluded that an axial dislocation is not essential for the growth of whiskers. This knowledge provided the initiation of the vapour-liquid-solid mechanism of filamentary single crystal growth put forward by Wagner and Ellis.³²

Vapour-Liquid-Solid Theory (V-L-S)

The basic postulate of this theory is that an impurity is necessary for crystal growth. The actual mechanism, however, is

very complex and the atomistic details are almost completely unknown. The theory proposes that the role of the impurity is to form a liquid droplet of relatively low freezing point. The molecules adsorbed on the surface of the substrate diffuse to the liquid alloy droplet. The impurity in the liquid acts as a catalyst, providing the chemical reduction to release the metal atoms. The liquid thus becomes supersaturated with respect to metal atoms and growth proceeds by precipitation of metal from the droplet. Since the whisker grows from the liquid, a screw dislocation is unnecessary.

For the specific case of copper whiskers the V-L-S mechanism would suggest the following sequence. Copper iodide molecules condense on the substrate or crystal sides and migrate by diffusion to the liquid at the tip. The liquid droplet is a copper iodide-impurity alloy which causes the catalytic reduction of copper iodide to copper. The liquid is then supersaturated with copper and copper precipitates, with a very small concentration of impurity in solid solution. The precipitation occurs at the interface between solid copper and the liquid alloy. By continuation of this process the alloy droplet becomes displaced from the substrate and remains atop the growing whisker, as shown in Figure 3.

During the catalytic decomposition of copper iodide to copper and iodine, the iodine vapour will be swept away by the gas stream

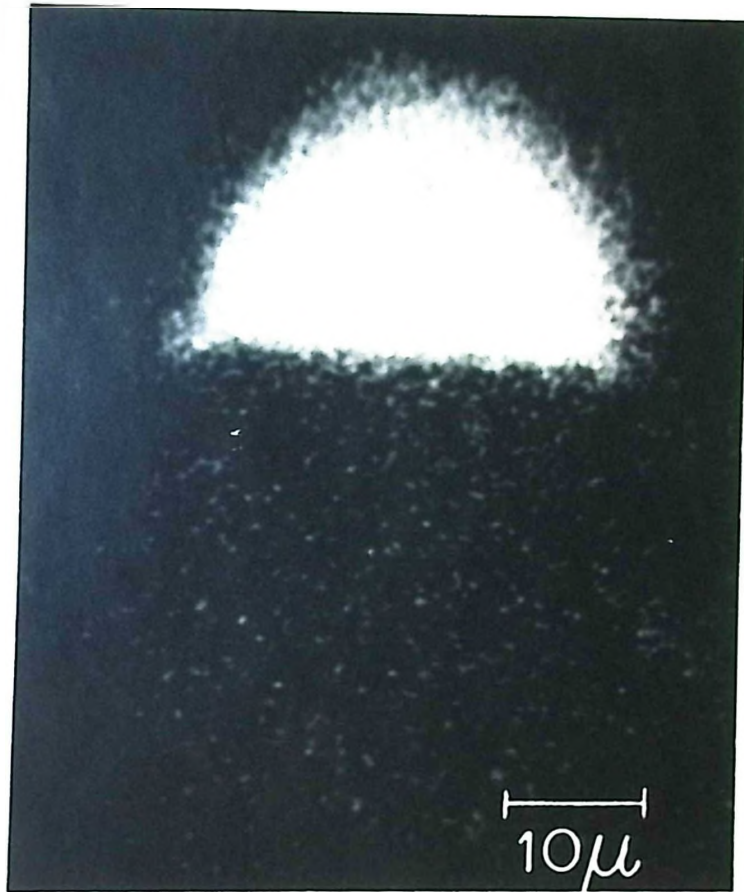


FIG. 3

ELECTRON-PROBE MICROGRAPH OF SILICON WHISKER
SHOWING GOLD IMPURITY (WETTED) SEGREGATED MAINLY AT THE TIP

(Courtesy W. C. Ellis, Trans. A.I.M.E. -- to be published.)

and condense on the cooler parts of the furnace tube. However, it is highly probable that some of the iodine will not manage to escape and become trapped in the copper lattice.

Since the crystals are cooled in a stream of hydrogen the impurities will have a tendency to segregate to the surface. Hence, when the whiskers are dissolved, they will exhibit different dissolution characteristics for their surface and for their bulk.

Working with iron whiskers, Seastrom, Beck and Fontana²³ did, in fact, find quite different morphological effects upon etching at various depths of the whisker. On etching the as-grown whisker the morphology was rough and irregular. However, once this outer "scale" was etched away the surface exhibited a smooth topography which remained smooth on successive etching.

Such effects are consistent with those found during this research. The initially irregular dissolution profiles are discussed more fully in Chapter VII.

CHAPTER III

THEORY OF DISSOLUTION

Introduction

The theoretical analysis of crystal dissolution can be divided into two categories: (a) those which invoke a mechanistic approach, as first applied by Burton, Cabrera and Frank,⁶ and (b) those based on kinetic arguments such as that formulated by Frank.¹³

The mechanistic theory employs the concept of a surface composed of singular-surfaced terraces separated by monatomic ledges lying in low index directions. The theory of Frank, however, is not dependent upon the surface model and may be regarded as a geometrical theorem which describes the profile of a changing shape.

Mechanistic Theory (B. C. F.)

The mechanistic theory of crystal dissolution was first proposed by Burton, Cabrera and Frank,⁶ and later modified by Cabrera and Levine³³ and Hirth and Pound.⁸ This theory is mathematically meticulous but will be reviewed here only in conceptual outline.

Regarding the surface as vicinal the dissolution process reduces to a diffusion problem with the ledges being diffusion sources a distance λ_B apart, where λ_B represents the characteristic displacement distance (as introduced in Chapter I). Since the mobility of the surface atoms is high then it is legitimate to neglect the motion of the ledges and consider only the motion of surface atoms.

The saturation ratio of a solution is given by $\frac{C}{C_0}$, and the degree of saturation by

$$\frac{C - C_0}{C_0} = \sigma \quad (16)$$

The flux of atoms leaving the surface of a metal depends on the mean displacement of an atom on the surface (λ_B), the maximum saturation of the metal in solution (C_0), the degree of saturation (σ), and the equilibrium number of atoms leaving per unit area:

$$\text{i.e. flux } j \propto \frac{\sigma \cdot \lambda_B \cdot C_0}{\sqrt{2\pi m k T}}$$

The exact expression is

$$j = \frac{2\sigma \lambda_B C_0}{\sqrt{2\pi m k T}} \quad (17)$$

where the factor 2 comes into the equation since atoms are being liberated both from right and left ledges.

If the volume of an adatom is denoted by Ω , and the height of a ledge by h , then the velocity of recession of a ledge is given by

$$V_{\infty} = \frac{2\sigma \lambda_s C_0}{\sqrt{2\pi} \sqrt{m k T}} \times \frac{\Omega}{h} \quad (18)$$

Assuming $\frac{\Omega}{h} = 10^2 - 10^5$ and taking typical values for a metal,⁹ gives

$$V = (10^{-2}\sigma - 10\sigma) \text{ cm/sec.}$$

This is the maximum steady state velocity that a step can attain, and is only achieved when the ledges are separated by a distance λ_s or greater. If the distance between ledges is smaller than λ_s then the diffusion fields interact causing the ledge velocity to be retarded. Under this circumstance the velocity of movement of the step is modified to

$$V(\lambda) = \frac{2 C_0 \lambda_s \sigma}{\sqrt{2\pi} \sqrt{m k T}} \times \frac{\Omega}{h} \times \tanh\left(\frac{\lambda}{2\lambda_s}\right) \quad (19)$$

As seen from this equation, as $\lambda \rightarrow 2\lambda_s$ then $V(\lambda) \rightarrow V_{\infty}$ i.e. the velocity again becomes the steady state velocity given by equation (18).

The slope of the dissolution trajectory* for any concentration

* The dissolution trajectory is the locus in space of a particular orientation of crystal surface and has important significance in the Kinematic Theory.

of solution C , is given by

$$P_c = \frac{2 C_0 \lambda_s \sigma}{(2\pi mkT)^{\frac{1}{2}}} \times C \times \tanh\left(\frac{h}{2 \lambda_s C_0}\right) \quad (20)$$

The mechanistic theory calculates the steady state dissolution velocity. However, experimental results show that the time required for the establishment of really steady state conditions is usually quite long, so that the dissolution process corresponds to transient conditions rather than steady state conditions.

The realization of this fact led, in 1958,³ to a treatment of the transient state of crystal dissolution to provide the foundation of the Kinematic theory of crystal dissolution.

Kinematic Theory of Crystal Dissolution

Frank³ (also Cabrera⁹) developed a continuum kinematic theory of step motion based on Lighthill and Whitham's³⁴ theory of traffic flow on highways. When the rate of dissolution depends only on step density, Frank's theory describes the orientation profile as dissolution proceeds and hence describes the kinetics of step spacing. The theory, as it will be developed, is two-dimensional referring to a layer of uniform thickness.

With reference to Figure 4 let k be the step density i.e. the number of steps per unit length in the region of a particular point; and q be the step flux i.e. the number of steps passing that point in unit time.

As seen from Figure 4,

$$hk = \text{surface slope} = \frac{\partial y}{\partial x} \quad (21)$$

and

$$hq = \text{normal dissolution rate} = - \frac{\partial y}{\partial t} \quad (22)$$

The theory then makes the basic postulate that the number of steps passing a point in unit time (q) depends only on the step density in the region of that point (k); or is dependent on time only through orientation--independent factors;

$$\text{i.e. } q = q(k)$$

From this postulate we arrive at two velocities. The first is the mean speed of an individual step, V

$$V = \frac{q}{k} \quad (23)$$

and the second is a velocity called the "kinematic wave velocity" given by

$$c = \frac{dq}{dk} \quad (24)$$

Now the two original parameters of density and flux can be related using the continuity equation,

$$\frac{\partial q}{\partial x} + \frac{\partial k}{\partial t} = 0 \quad (25)$$

$$\begin{aligned}
 * \quad \frac{dq}{dk} \cdot \frac{\partial k}{\partial x} + \frac{\partial k}{\partial t} &= 0 \\
 \frac{dk}{dt} &= \text{Const}(c) \frac{dk}{dx} \\
 \frac{dk}{dx} \cdot \frac{dx}{dt} &= c \frac{dk}{dx}
 \end{aligned}$$

Hence

$$\frac{dx}{dt} = \text{Constant } (c) \quad (26)$$

i.e. in the (x,t) plane the crystal slope is constant with time. Such a line is called a "characteristic". Thus once the crystal starts to dissolve it continues to dissolve with a constant or "characteristic" slope.

Further, the sequence of slopes in the (x,y) plane may be deduced.

$$\begin{aligned}
 y &= y(x,t) \\
 dy &= \frac{\partial y}{\partial x} dx + \frac{\partial y}{\partial t} dt \\
 \frac{dy}{dx} &= \frac{\partial y}{\partial x} + \frac{\partial y}{\partial t} \cdot \frac{dt}{dx} \\
 &= hk + (-hq) \cdot \frac{1}{c} \\
 &= h \left(k - \frac{q}{c} \right) \quad (27) \\
 &= \text{Constant} \quad (28)
 \end{aligned}$$

* The change from partial to full derivatives is permissible owing to the explicit dependence of q on k only.

From the above calculations, where the dissolution (or growth) velocity is defined as measured normal to the macroscopic surface of the crystal, rather than normal to the crystallographic terraces, Frank³ introduced the basic theorems of the Kinematic Theory of crystal dissolution (or growth).

Theorem I: The rate of dissolution of a crystal surface is a function only of orientation (or depends on time only through orientation-independent factors) the locus in space of a particular orientation of crystal surface on dissolution is a straight line. Further, the orientation dependence of the etch rate allows the dissolution properties of a crystal in a given solvent to be described in terms of a polar diagram of the reciprocal normal etch rate as a function of orientation (the Reluctance Diagram).

Theorem II: The vector defining the locus in space of a given crystal surface orientation is parallel to the normal drawn from the reluctance surface at the corresponding orientation.

Thus points of a given orientation on the (x,y) plane have straight line trajectories and it follows that they are also straight on the (x,t) and (q,t) planes. These concepts are summarized in a geometric construction given in Figure 5, showing the direction of a trajectory of a point of given orientation.

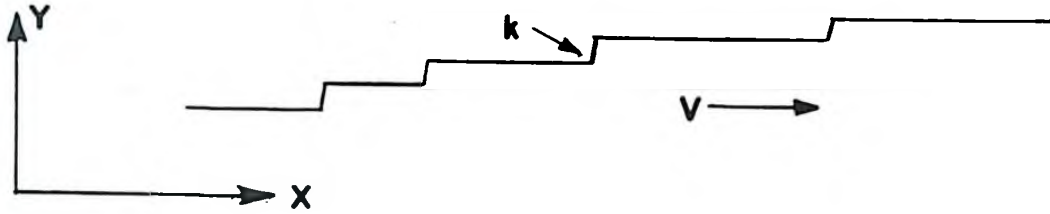


FIG 4
STEPS ON CRYSTAL FACE

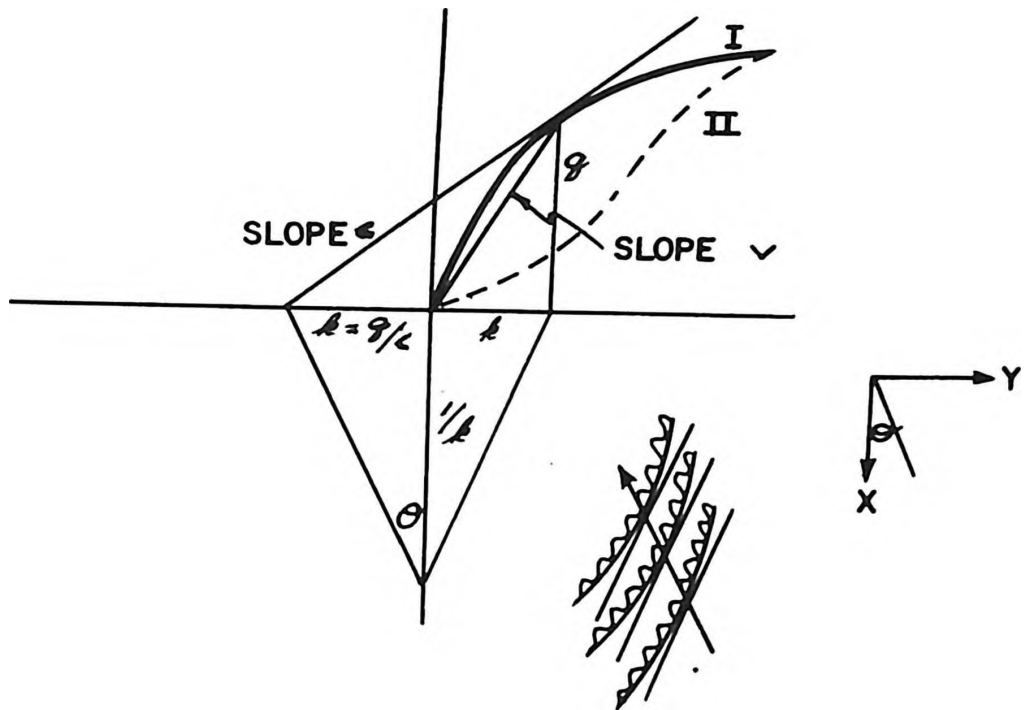


FIG 5

RELATIONSHIP BETWEEN STEP FLUX (g) AND STEP DENSITY (k),
AND GEOMETRICAL CONSTRUCTION OF ORIENTATION TRAJECTORY

Two types of dissolution dependence are drawn in Figure 5 and denoted by I and II. A curve of type I corresponds to growth of a crystal under high purity conditions. A wave of type II is thought to correspond to the case in which impurities interfere with the motion of steps.

Theorems I and II have been verified experimentally by Frank and Ives³⁵ for the dissolution of germanium and by Ives³⁶ for lithium fluoride. Ives and Hirth³⁷ found that dissolution at dislocation etch pits in lithium fluoride dissolving in a dilute solution of ferric fluoride did not follow the kinetic laws predicted by Frank's theory or by the approach of Burton, Cabrera and Frank. However, their results were consistent with the mechanistic theory if a time-dependent adsorption of ferric-fluoride poison at the receding steps was invoked.

Frank³ investigated the profiles of step bunches in accordance with his theorems. These considerations are illustrated schematically in Figure 6. The characteristics for low values of k have smaller slopes than those for high values of k (equation 27), so that at the leading edge of the bunch the characteristics diverge. At the trailing edge they converge and ultimately meet. At the point of intersection, the intervening density values vanish and a discontinuity in density develops. At a later time (t_1) the step bunch has assumed the density distribution $k(x_1, t_1)$.

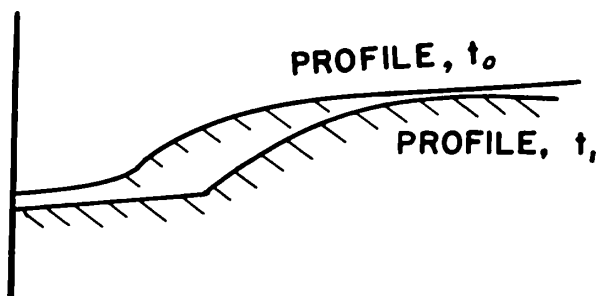
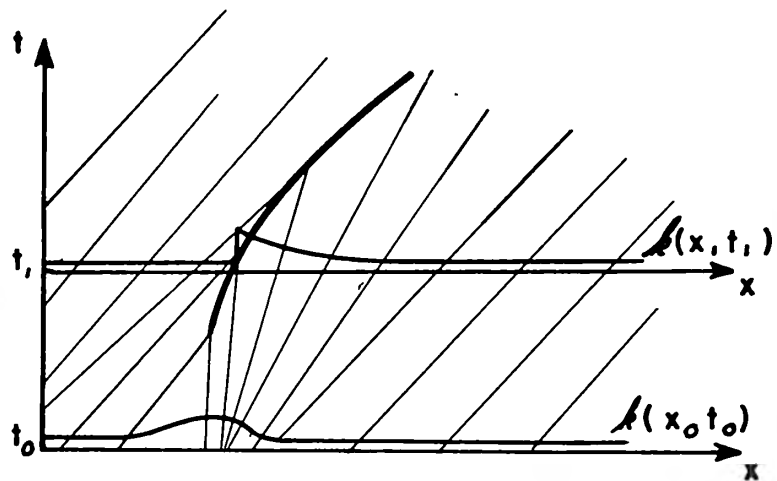


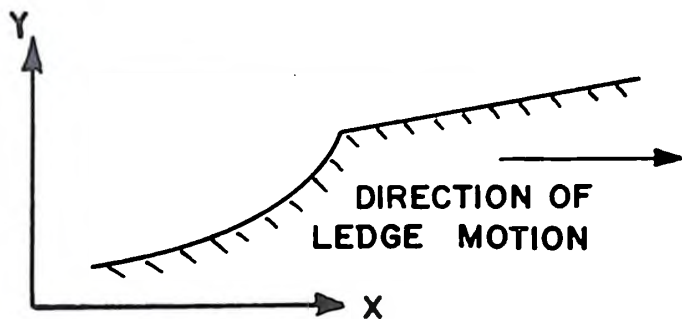
FIG 6

PROGRESSIVE DISPLACEMENT AND CHANGE OF SLOPE
OF A STEP BUNCH

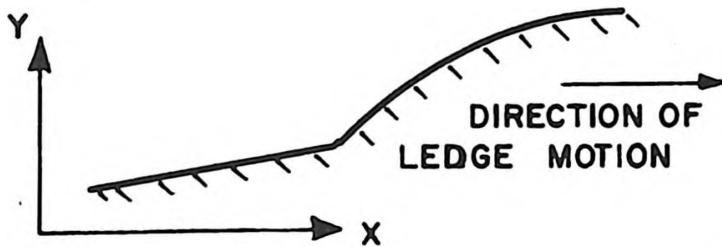
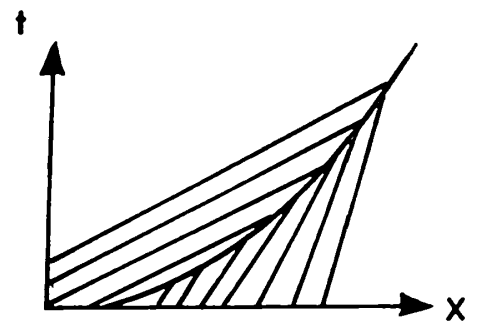
Frank's theory results in a discontinuity in slope at the rear of a step bunch for any initial profile, with an increasingly rounded leading edge as long, as $\frac{d^2q}{dk^2}$ is negative (Figure 5). In order to develop a macroscopically resolvable profile (as in an etch pit) $\frac{d^2q}{dk^2}$ must be positive, i.e. Figure 5 must be of type II. Frank states that "when q depends on k in the simplest way, by interference through the diffusion fields of neighbouring steps, this cannot occur except for very steep slopes, approaching other low-index surfaces."

The necessary reversal in the curvature of the q versus k plot can be accomplished through the effects of impurity on $q(k)$. The impurity species must satisfy certain criteria viz., that its concentration be low in order to exhibit a time-dependent surface adsorption requiring a very long time to reach equilibrium, and that it can be removed by the passage of a step. In this way, the adsorbed impurity inhibits the propagation of dissolution steps across a surface, the reduction in step velocity being a function of the preceding terrace width. This is a self-accentuating phenomenon since the density of adsorption met by an oncoming step is an increasing function of the time lapsed since the passage of the previous step (i.e. $\frac{1}{q}$).

If $\frac{dq}{dk}$ is positive, steps are more impeded by the impurity effect when they are widely separated than when they are in close



(A)



(B)

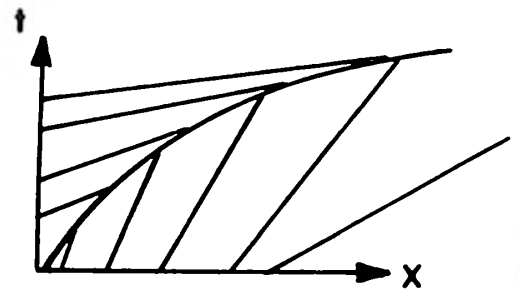


FIG 7

SCHMATIC ILLUSTRATIONS OF PROFILE DISCONTINUITIES RESULTING FROM STEP BUNCHING WITH CORRESPONDING TIME/DISTANCE CURVES

(A) POSITIVE $\frac{d^2q}{dk^2}$

(B) NEGATIVE $\frac{d^2q}{dk^2}$

proximity. It is this effect which can make a positive contribution to $\frac{d^2q}{dk^2}$, reversing the curvature of the crystal surface.

For small values of k , i.e. vicinal surfaces, $\frac{d^2q}{dk^2}$ has only a small negative value. Therefore, for vicinal surfaces, a very slight impurity effect can suffice to transfer the discontinuity from the rear to the front of the bunch.

So far, it has been established that the two possible surface profiles are as shown in Figure 7. However, to date all surface studies reveal only type (A). A possible explanation for this may be postulated with reference to distance versus time graphs (Figure 7). Note that in type B, for a small time interval, the distance travelled by the shock wave is very large. Hence, although it occurs it could be that it is too fast to be observed. However, in type A, the distance travelled in a time interval decreases with increasing time, and so the shock wave is retarded causing bunching, observed in the form of a pit.

Kinematic Theory Applied to
Macroscopic Symmetry Sections

So far, mention has only been made to the microscopic bunching of steps and how this may result in localised pitting. Theorems I and II are, however, equally applicable to considerations of the

total crystalline volume. In fact, the theory was originally tested on bulk crystals.^{35,36}

In Chapter I, it was pointed out that the equilibrium shape of a crystal can be obtained via the Wulff Plot. If the equilibrium shape is known and all its orientations determined, then a polar reluctance diagram can be deduced, provided one has a knowledge of the etchant chemistry of the system.

For the particular case of copper whiskers the growth behaviour obeys the dictates of thermodynamics and crystallography. Both these frameworks impose certain restrictions on the growth shape. As an example, consider a crystal which grew under equilibrium conditions and developed six lateral sides. If this crystal grew in the direction of greatest atomic packing (i.e. $[111]$ for copper) then a standard stereogram shows these six sides to be $\{110\}$ or $\{112\}$. Reference to the Wulff Plot for this system would give both the surface energy values for the $\{110\}$ and $\{112\}$ orientations. The orientation with the smaller value would therefore be the external face.

In the same way as the Wulff Plot allows the construction of the "equilibrium growth shape," the reluctance diagram allows the "equilibrium dissolution shape" to be determined. In this respect there is a qualitative connection between the Wulff diagram and the reluctance diagram. Although a 1:1 correspondance does not

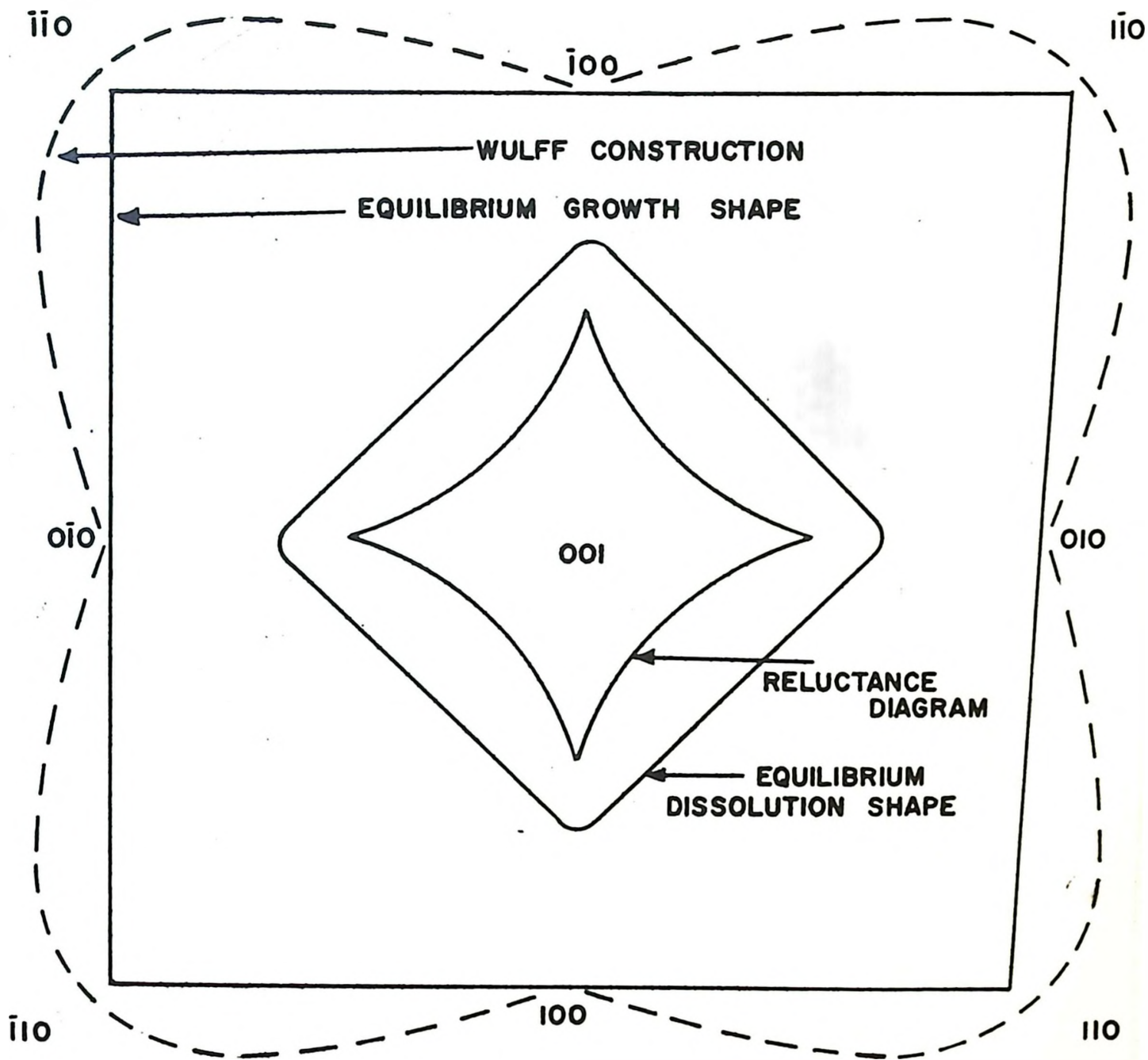


FIG 8

WULFF CONSTRUCTION AND DEDUCED EQUILIBRIUM GROWTH SHAPE FOR A TWO-FOLD AXIS OF SYMMETRY. RELUCTANCE DIAGRAM AND EQUILIBRIUM DISSOLUTION SHAPE ARE ALSO SHOWN. (ONLY MAXIMUM AND MINIMUM CUSPS ARE SHOWN)

exist, an orientation with a high surface energy will etch faster, and so appear as a low value on the reluctance diagram. Values of the normalised etch rate for particular orientations give the reluctance diagram.

The interconnection between both diagrams is shown qualitatively in Figure 8. The constructions are not drawn to scale but the plots are normalised to illustrate the equivalence between surface energy and reciprocal dissolution rate. The "equilibrium dissolution shape" has been drawn with rounded corners corresponding to sharp maxima in the reluctance diagram. This is to illustrate that for the case of macroscopic dissolution, sharp points are smoothed out by the etchant leaving the general equilibrium appearance.

Even if the equilibrium shape is not attained, close packed faces will always tend to dissolve more slowly than kinked and ledged surfaces.

Criticism of the Theory

Detailed studies of the profiles of etch pits performed by Ives and Hirth³⁷ show the existence of curved etch pit profiles. This deviation from linearity is due to the assumption that the step flux depends only on the step density. Such an assumption

requires that the strength of the dissolution source remains the same for all times, which may not be necessarily so.

Such experimental data can be explained within the framework of the theory by introducing in the step flux (q) an explicit dependence on the distance (x) and the time (t). Unfortunately, if this were to be attempted the present method would break down.

A further criticism is that Frank's kinematic theory deals only with average step density. Although it explains the behaviour of fluctuations in step spacing once they have formed, it does not explain the initiation of atomistic perturbations set up during dissolution. Recently, Mullins and Hirth³⁸ have formulated the theory to include fluctuations in step spacing.

In this work, step motion is described by a system of differential equations, each one corresponding to a step interval, and describing the motion of steps in diffusion controlled dissolution. Their treatment agrees with the continuum kinematic theory to first order but there are important discrepancies when there occur sharp differences between the behaviour of alternate steps. For example, Mullins and Hirth³⁸ consider a train of four steps and show that it will break up in a pairwise grouping, with the leading pair escaping the trailing pair, and the trailing pair collapsing to a double step height.

Comparison with Experiment

There have been a number of experimental observations³⁹ of dissolution rates which confirm that the mechanism invoked is a diffusion controlled process. In other aspects of the theory, experiment is more conflicting. Some researchers⁴⁰ claim that etching rate does not depend on orientation, while others^{37,41} claim that the etching rate is not necessarily constant during the process.

However, there has not been much work carried out pertaining to small groups of steps but mainly with continuous trains of steps.

Very recently, a substantial advance in the experimental approach to dissolution has been made by the careful work of Young⁴² and coworkers at Oak Ridge National Laboratory. This group have performed a long series of experiments on the dissolution kinetics of copper single crystals in various etchants, culminating in the establishment of q/k waves (designated in their work as J/ρ curves). An example of such a plot is shown in Figure 9. As seen from this graph they can predict and control the ledge kinetics by manipulation of the etchant chemistry and the current density. For example, by fixing the current density and changing the ion concentration they were able to create and annihilate macroscopic ledges reversibly.

STEP FLUX VERSUS STEP DENSITY CURVES FOR DISSOLUTION IN SOLUTIONS OF VARYING BROMIDE ION CONCENTRATION
(AFTER YOUNG AND HULETT)

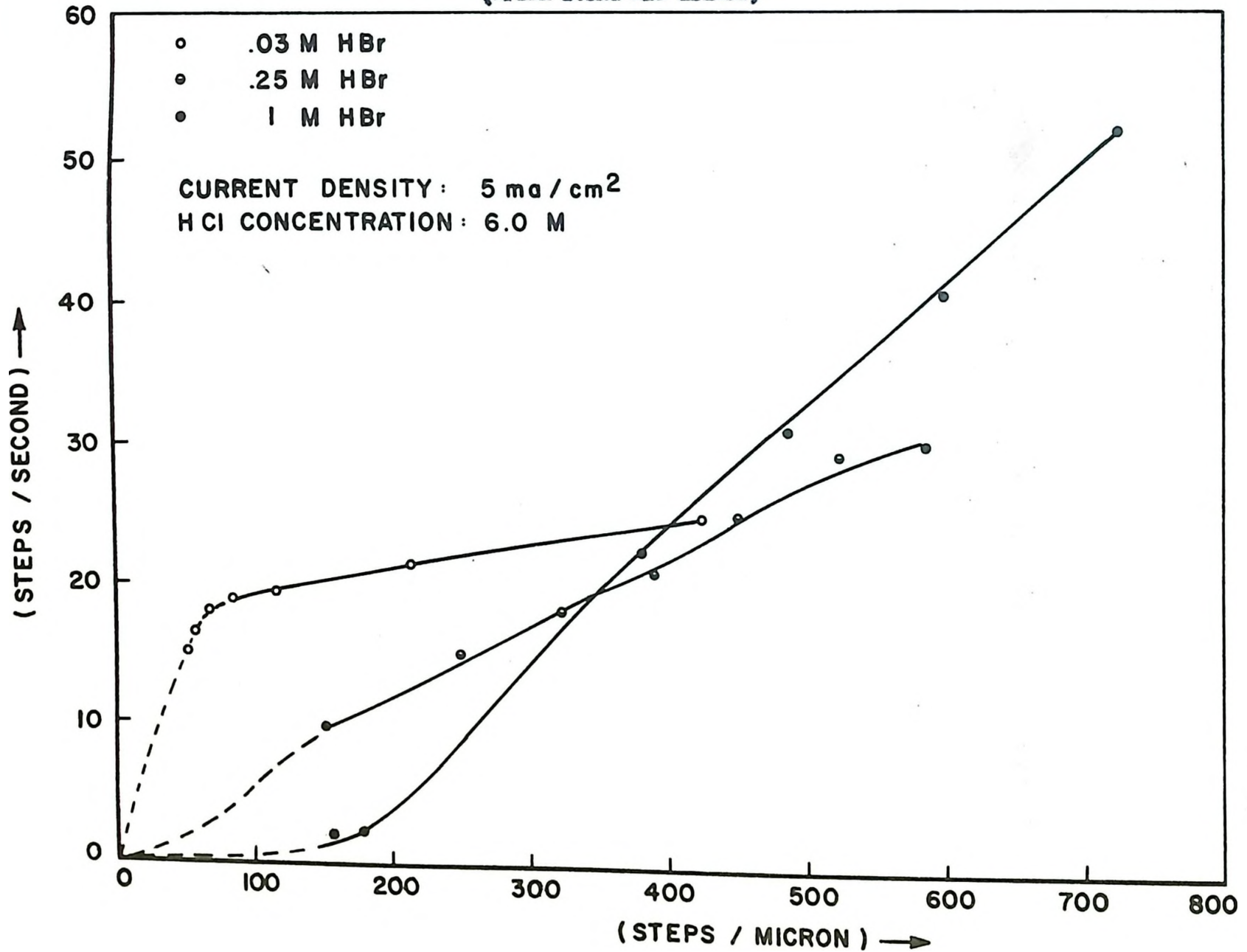


FIG 9

They also showed that the slope of the pit changed drastically with change in current density. This behaviour is consistent with that expected, if changing the current density from low to high values results in changing the q/k curve from type II to type I.

The importance of these experimental investigations cannot be overestimated since they show a complete control of dissolution mechanics by experimental parameters.

CHAPTER IV
FILAMENTARY GROWTH

Experimental Procedure

The apparatus for the growth of copper filamentary crystals was first used by Brenner⁴³ and is shown in Figures 10 and 11.

It consists of a "Hoskins-type" tube furnace containing a silica tube. The furnace is heated by $\frac{1}{2}$ " electrical resistance wirings and has a power input capable of 550 Watts via a 110:15 step down transformer. The basic electrical circuit is shown in Figure 11 (b). The temperature is measured by a chromel-alumel thermocouple and maintained by a thermoelectric "Tencometer". The gas flow rate is measured by a capillary flowmeter and controlled by a needle valve.

In operation, the furnace is heated to 650° C and the system flushed with helium (purity 98.9%). A fireclay boat containing copper iodide (purity 99.99%) is placed in the cool part of the furnace and allowed to preheat slightly for five minutes. With the helium still flowing the boat is pushed into the hot zone of the furnace. The helium is replaced by a flow of hydrogen (impurity 1 P.P.M.) of 100 ccs. per minute. Both gases are used direct from the cylinders

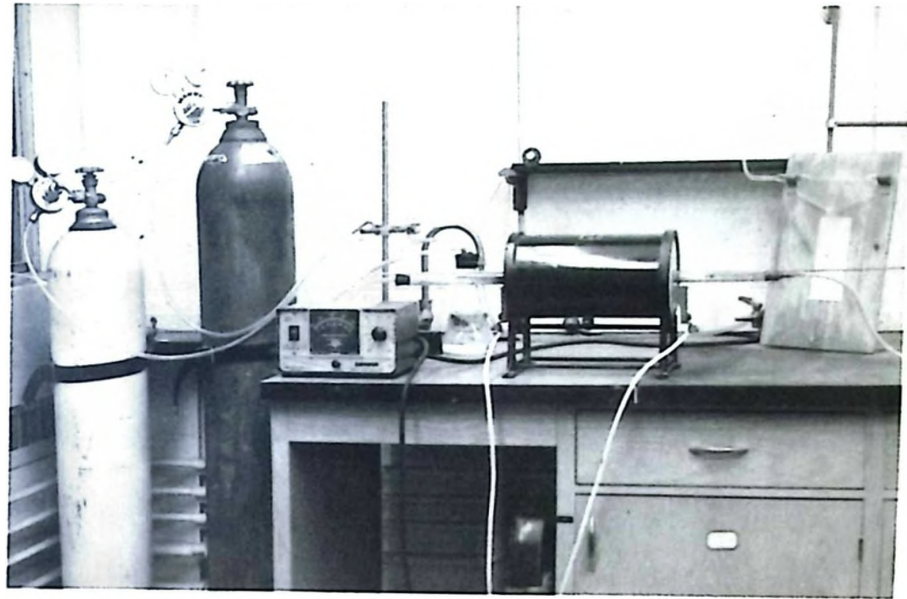


FIG. 10

APPARATUS USED FOR GROWING COPPER WHISKERS

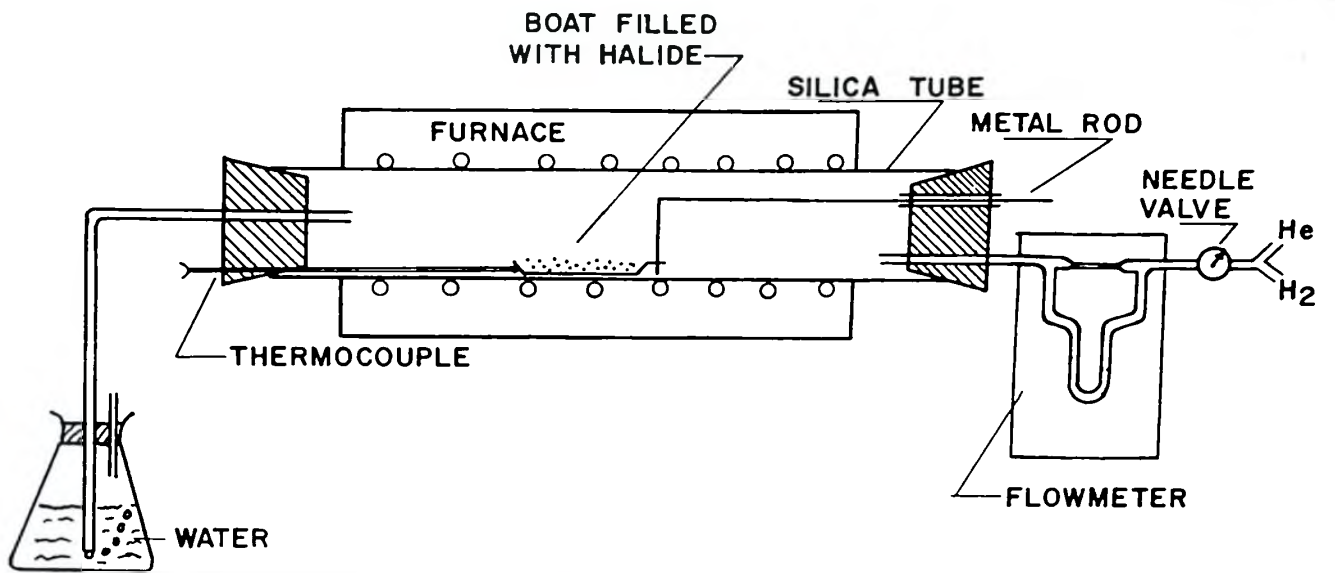


FIG II (a)

SCHEMATIC ILLUSTRATION OF WILSMER GROWING APPARATUS

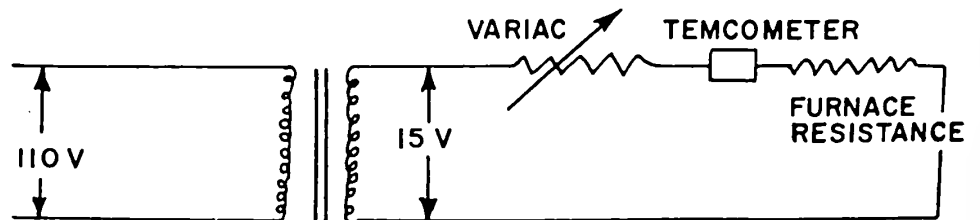


FIG II (b)

CIRCUIT DIAGRAM OF APPARATUS

and were not pre-heated. The rating of the furnace is sufficient to bring the boat and halide to the growth temperature within minutes; otherwise reduction takes place at too low a temperature. The gaseous products are bubbled through water to separate the poisonous hydrogen iodide.

After approximately fifty minutes the furnace is switched off and the boat is allowed to cool in a stream of hydrogen to prevent any high temperature oxidation, and also in an attempt to reduce any impurities on the crystal sides. On cooling, the temperature is maintained at 300° C for about an hour to enhance impurity removal. Although this last step is an addition to Brenner's technique it was considered necessary owing to the irregular dissolution profiles. After the anneal, the boat is pulled out to the cool zone and allowed to cool to room temperature in helium. The boat of crystals is then stored in a desiccator.

Variables in the Growth Process

When growing whiskers, there were runs which yielded a large bunch of crystals and other runs which produced nothing. This necessitated a systematic study of the variables involved in the growth process. Parameters involved were (1) nature of the substrate, (2) temperature, (3) pressure, (4) amount of halide added, (5) turbulence.

(1) Substrate. "Compax" fireclay boats were used to grow the crystals and it was found that used boats produced many more crystals than a new substrate of the same material. Fireclay boats which had successfully grown crystals would continue to yield positive results when mechanically cleaned and reused. However, if the same boats were thoroughly chemically cleaned (in hot nitric/hydrochloric acid) to give a smooth surface, they again produced no crystals, although all other conditions of growth were the same.

Metal boats were capable of producing finer crystals but of very much smaller quantities than a ceramic substrate. A fireclay boat which was half lined with metal strips grew crystals on the ceramic portion but none on the metal part. A ceramic boat which was half chemically cleaned using hot concentrated nitric acid and half mechanically cleaned, grew no whiskers on either half.

(2) and (3) Temperature and Pressure. Crystals grew in the temperature range 590°C (the melting point of copper iodide) to 680°C , and at flow rates of 50-300 cc/min. These ranges are the same as those cited by Brenner.⁴³

(4) Amount of Halide Added. A boat half-filled with halide seemed the optimum for producing good whiskers. Too much copper iodide present resulted in an entanglement of crystals. Such conditions also affected the growth of a single crystal, causing a large proportion of kinked and twisted shapes.

(5) Turbulence. It was observed that boats of crystals only grew when the tube was dirty. It was thought that the dirt caused interference of the gas-flow, making turbulence a necessary condition of growth. When the tube was thoroughly cleaned and a block of silicon inserted in front of the boat to create further turbulence, still no crystals grew. This was repeated four times, the furnace tube gradually becoming dirtier each time. A few crystals were obtained in the fourth boat. Further boats produced more and more crystals.

When whiskers were being successfully grown the furnace tube was replaced by a new one. No crystals were obtained. On continuing growth runs (and in the process "Breaking-in" the tube), gradually whiskers would be successfully grown. Since all other conditions were the same in each case, this would suggest that impurities in the tube are an essential condition for whisker growth.

In the light of the above, it would appear that the necessary conditions for the growth of copper whiskers are as follows:

- (1) Temperature: 590° C - 680° C
- (2) Amount: $\frac{1}{2}$ full with halide
- (3) Flow Rate: 50 - 300 ccs./min.
- (4) Time: 45 minutes
- (5) Substrate: Reused ceramic boats
- (6) Furnace Tube: Reused silica tube

Handling of the Whiskers

Whisker research is greatly hampered by the extreme experimental difficulty of handling crystals that are sometimes only a few microns thick. The crystals grown varied in length from .1 mm - 2 cms and in diameter from .1 - 50 microns. The crystals were plucked at their base from the boat and handled using Dumont precision forceps. Mishandling gives rise to slip and deformation bands, shown in Figure 17.

Analysis

The inconsistent results of whisker dissolution necessitated an analysis of the crystals. A neutron-activation analysis was performed on two boats of crystals and the average impurity content calculated in Appendix II.

CHAPTER V

DISSOLUTION EXPERIMENTS

Introduction

A crystal of high surface reflectivity and not too thick was plucked by its base from the boat. The forceps were then clamped with an elastic band in preparation for the whisker becoming the anode of an electrochemical cell. The cathode of the cell was also a whisker, i.e. of the same dimensions as the anode. A large copper cathode had been used for the preliminary runs, but this was discarded since it did not provide zero potential on open circuit.

Considerable time was expended on the establishment of the optimum electrolyte composition. Initially, following Saubestre,⁴⁴ a dilute solution of ferric chloride in distilled water was tried. This resulted in uncontrollable pitting giving a rough attack at even the lowest current densities. Following Young,⁴² an electrolyte consisting of hydrobromic and hydrochloric acid was employed. Dissolution in this system caused all the crystal surface to be etched, even parts above the solution surface, due to the

high vapour pressure of bromine. Although it was attempted to partially cover the crystal, etch and then dissolve off the protective covering, successful attempts were few. Surface tension and wettability of the liquid plastic, exfoliation of the plastic film coupled with the difficulty in removing it, were responsible for the failure of this method. A 1-N solution of sulphuric acid provided controllable dissolution, but it was found that the weight of dissolved copper was many orders of magnitude smaller than that predicted by Faraday's second law. This discrepancy was due to the transport in the cell being affected by electrons and not copper ions from the anode. This difficulty was circumvented by adding analytical grade copper sulphate to the electrolyte, thus ensuring that all transport was ionic. With the electrolyte of .2 Molar copper sulphate, 16% sulphuric acid, undersaturation of .513 and pH of 2.3, the cell efficiency was experimentally found to be between 95 - 98%.

Cell efficiency is normally determined gravimetrically. However, when dealing with crystals weighing approximately one microgram, such a technique is out of the question. The cell efficiency was therefore found by selecting a crystal, measuring its width along its length on a Reichert microscope, etching at a definite current for a definite time, re-measuring the width at

the same positions as before and hence calculating the volume removed, assuming the crystal is a cylinder. The volume is then converted to the weight dissolved and this value compared with the theoretical value obtained using Faraday's second law.

The electrolyte was de-aerated with purified nitrogen for an hour before each dissolution experiment since it was found that oxygen present set up local cell action causing a pitting attack. The nitrogen was continued bubbling during the experiment.

The Apparatus

Owing to the exceptionally small dimensions of whiskers, dissolution experiments at low current densities necessitate operational currents in the region of 10^{-7} - 10^{-9} amps. To measure currents of this order of magnitude use was made of a Keithley 610A Electrometer having a range of 10^{-1} - 10^{-13} amps.

For the study of dissolution cross-sectional shapes, a micrometer device was constructed (Figure 12). The micrometer scale is divided into one hundred divisions, each division giving ten microns movement. Although the backlash of the screw was greater than ten microns, movement took place only in one direction so that this source of error is not relevant. Holes were drilled on both sides of the machine on two inch centres. This enabled the micrometer to be screwed into a constant position on a Vickers

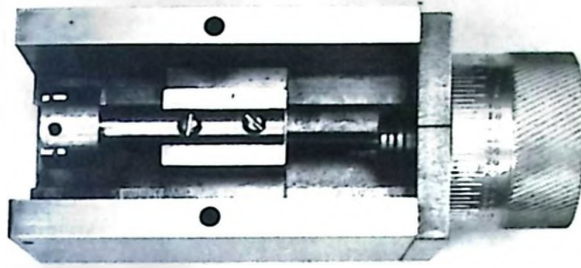


FIG. 12
MICROMETER DEVICE



FIG. 13
MICROSCOPE STAND

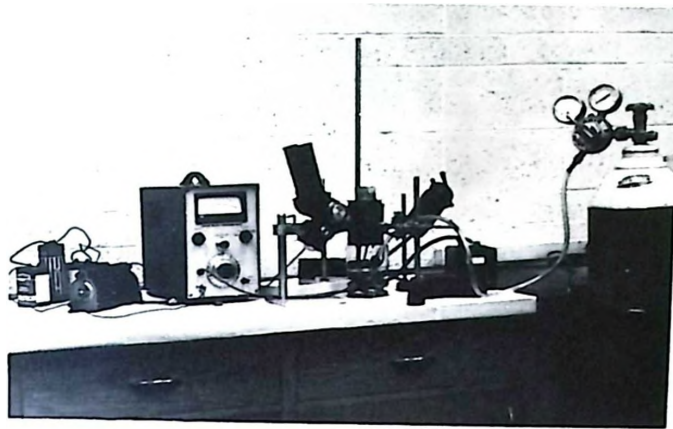


FIG. 14

APPARATUS USED FOR DISSOLUTION

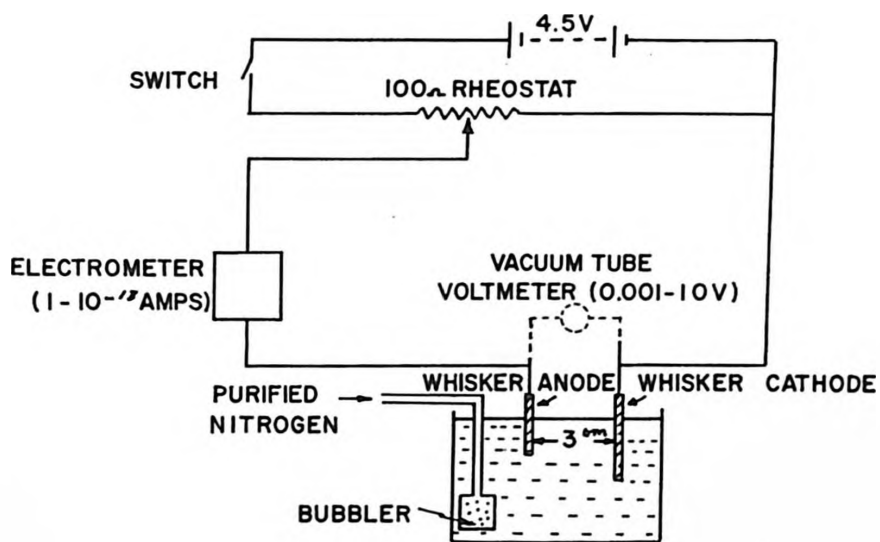


FIG 15

SCHEMATIC REPRESENTATION OF DISSOLUTION ASSEMBLY

microscope stage, which also has holes tapped on two inch centres.

This design permitted step-wise dissolution to be performed and measured, and the resulting cross-sectional shapes to be related to the step-wise dissolution. A stand -- Figure 13 -- was used to carry a stereo-microscope thus allowing observation of the dissolving crystal.

The complete assembled apparatus is shown in Figure 14, with the electrical circuit sketched in Figure 15.

The experiments performed may be broadly grouped into two classes; those concerned with surface examination and those concerned with cross-sectional examination.

Surface Examination

In all experiments where the examination of the surface was of prime importance, the micrometer device was not used.

For surface examination, a crystal was selected for its high reflectivity and placed on a glass slide. Owing to the electrostatic attraction between copper and glass, and the fineness of the crystal, the slide could be turned upside down without the crystal falling off. The slide was placed on the Reichert microscope and, using the 85X objective, with the tip as a

reference point, the width of the crystal was measured along its length. The crystal was then taken from the slide with precision forceps ready to be dissolved.

The crystal was mounted close to the surface of the electrolyte and the whole bath was raised by a Jack Stand, until greater than half the anode was immersed. The current was then switched on and the stop watch started. Usually a slight manipulation of the rheostat was required to bring the current to the proper value. The current was either maintained at a constant value or, when operating at a constant current density, decreased by pre-determined amounts.

After a pre-determined time the current was switched off, the etched whisker removed and dipped into distilled water to remove any traces of electrolyte. It was then placed on a slide and its unetched end glued to the slide using a solution of vinyl chloride in methyl ethyl ketone. The slide was returned to the microscope and the length of the etched crystal measured. In this manner the area of the crystal etched could be calculated.

Where data on the current density versus cell potential was required, a vacuum tube voltmeter of 100 mega-ohm impedance was inserted into the electrical circuit as shown -- Figure 15. The resistance of the cell was measured with the electrometer to be 5×10^5 ohms. Hence, the impedance of the voltmeter distorts the

current reading by less than 1%, which is of the same order as the intrinsic noise of the electrometer.

By slowly decreasing the variable resistance, the current through the cell could be increased, with a corresponding change in potential across the cell.

The surface was examined on a Reichert microscope under oil immersion and photographed using 35 mm Panatomic X film. The film was developed using Microdol developer for 7 minutes at 68° F and printed using Leonar extra hard paper.

Cross Sectional Examination

A selected crystal was plucked by its base from a numbered boat with forceps and mounted in preparation to becoming the anode of the electrolytic cell. A two cm. square of acrylic sheet was cut and a slot approximately 1.5 cm long and .5 cm wide was positioned near one end. This end was then thinned down to wafer thickness.

The crystal to be dissolved was placed across the slot and fixed to the slide by dabs of silver print at both ends. The connection was tested using a Universal meter and, after continuity had been established, the basal end of the slide was coated with a liquid plastic ("Microstop"), to prevent any dissolving of the silver print. The slide was then clamped into position on the

micrometer and the machine inserted into the circuit as shown in Figure 14.

The solution was raised by means of a jack until it came close (but not touching) the micrometer. The difference between the level of the electrolyte and the bottom of the micrometer was measured and this difference added to all subsequent dissolution measurements. This was necessary since the high surface tension of the electrolyte caused it to climb up the micrometer, destroying the reference bottom of the machine. Attempts at reducing the surface tension of the electrolyte by adding fatty acids were unsuccessful since the oils were immiscible in acidified copper sulphate.

The micrometer was then adjusted until the crystal was in contact with the electrolyte and the reading noted. The current was switched on to a set value and the stop-watch started.

After a known number of coulombs had passed, the crystal was lowered a measured amount. The current continued to pass for a certain predetermined time and then the electrolyte lowered to expose the crystal.

By this method of lowering the crystal into the solution at fixed intervals, the whisker was therefore dissolved in a step wise-manner. Thus the width and cross-sectional shape of the whisker changed at definite intervals along its length.

Brenner and Morelock⁴⁵ quote a thermosetting plastic as the mounting material they used for cross sectioning whiskers. It is

preferable, however, to use a cold setting material so as not to disturb the whisker setting. "Polyite" mounting material was used to satisfy this criterion. It also has the advantages of being cold setting, pore-free, does not expand on solidification and is transparent, so that the whisker may be observed in the mount.

The whisker was then polished on 400 silicon carbide paper until the edge of the slide appeared. From then on it was polished through 600 paper 6μ and 1μ pads and 0.3μ alumina vibratory polisher. In this manner, the cross section observed was considered to be undistorted by the mechanical polishing.

The mount was polished to the corresponding readings as noted during the dissolution experiment. Examination took place on the Reichert with the slide holding the crystal always at right angles so that the successive shapes could easily be correlated. The cross-sectional shapes were photographed with a 35 mm Asahi Pentax.

Correlation of Cross Sectional Shapes

Following a method by Sunquist⁴⁶ it was possible to determine the amount dissolved from a particular orientation by measuring the width change of the crystal through 180 degrees. An acrylic board was machined into a circle and graduated into 360 degrees. Vernier

calipers were fastened to the board and the assembly could be rotated about a central pin as shown in Figure 16. The photographic negative of the cross-sectional profile was placed in the enlarger and its outline measured through 180 degrees. This was repeated for the successive dissolution shapes. Since each degree corresponds to a particular orientation, the width difference between two successive dissolution profiles at the same angular measurement gives twice the amount dissolved from that orientation. This was then divided by the time to give the dissolution rate for that particular orientation.

Crystals were etched at different current densities since whiskers from different boats showed different current/potential relations. Thus all crystals from one boat were etched at one current density, which could be different from that corresponding to another boat. Dissolution at varying current densities leads to a more difficult interpretation of the results, but, a crystal was dissolved at the current density dictated by observations of other etched crystals from the same boat.

Although etching had been performed at different current densities, all dissolution rates were converted to a rate corresponding to a current density of 1.5 micro-amps for comparison purposes.

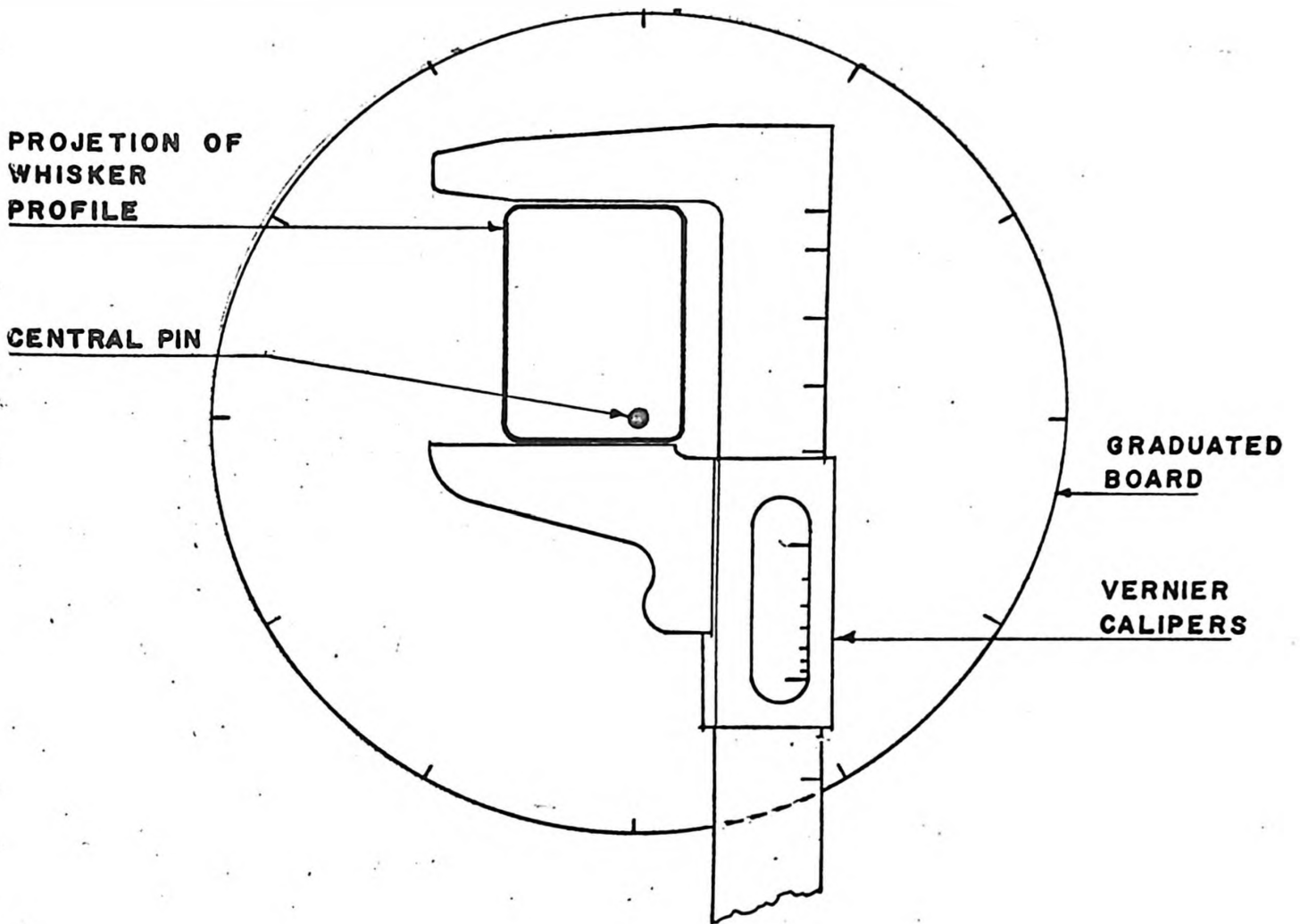


FIG. 16

CONSTRUCTION FOR DETERMINING THE AMOUNT DISSOLVED FROM EACH ORIENTATION

Justification for such a normalisation depends on the same dissolution mechanism holding over the range of current densities used. This is considered to be so on the basis of surface morphologies obtained over a range of current densities. Surface morphologies obtained over a range of 3 - 10 μ amps/sq. cm. are shown in Figure 19 and from these photographs the dissolution mechanism is considered constant over this current density range.

Once the etching rates had been established for fixed experimental conditions, the average etching rate for the $\{100\}$, $\{111\}$, $\{112\}$ and $\{123\}$ orientations was calculated.

CHAPTER VI

RESULTS

Growth

The experimental growth parameters of temperature, flow rate, substrate, time and amount of halide, were varied and the results noted. For each boat of crystals produced, measurements were made of the length and width of a representative sample of 10% of the total quantity. This permitted an estimate of average length and average width for various growth conditions.

A general appraisal was made of the average whisker condition as to whether they had highly reflecting or dull surfaces, were kinked and twisted or straight, and broad or fine. This information is given in Table I.

During growth, the macroscopic conditions were maintained constant, except in one case where the flow rate was varied. In general, most of the crystals were straight, many being uniform along their length, while some were uniform over part of their length then tapered to a point.

TABLE I

Boat Number	CONDITIONS OF GROWTH						RESULTS OF GROWTH			
	Temperature (°C)	Flow Rate (cc/min.)	Substrate	Time	Amount	Other	Quantity	Average Length (cm)	Average Diameter (μ)	Comment
1	650	100	New Ceramic Boat	1 hour	1/2 filled	Boat Preheated	nil			
2	660	75	New Fireclay Boat	50 mins	1/2 filled		2	.5	10	Poor appearance
3	640	75	Old Fireclay Boat	50 mins	1/4 filled		30 (Approx.)	.5	10	Poor appearance
4	640	50	Old Fireclay Boat	55 mins	1/4 filled		30 (Approx.)	.75	20	Good surface appearance
5	640	100	Old Fireclay Boat	50 mins	1/2 filled		20 (Approx.)	.75	20	Many kinked and twisted
6	625	100	Old Fireclay Boat	60 mins	1/2 filled		30 (Approx.)	.75	20	Reasonable surface appearance
7	625	100	Old Fireclay Boat	50 mins	1/2 filled		100 (Approx.)	1.5	25	General surface appearance good. Crystals entangled with one another.

TABLE I (cont.)

Boat Number	CONDITIONS OF GROWTH						RESULTS OF GROWTH			
	Temperature (°C)	Flow Rate (cc/min.)	Substrate	Time	Amount	Other	Quantity	Average Length (cm)	Average Diameter (μ)	Comment
8	640	100	Old Fireclay Boat	56 mins	1/2 filled		500 (Approx.)	1.5	25	As in 7
9	640	100	Fireclay Boat	50 mins	1/2 filled	New Boat	3	.75	10	Very badly twisted
10	650	100	Old Fireclay Boat	55 mins	1/4 filled		50 (Approx.)	.5-1	5	Very fine crystals but badly deformed
11	650	100	Old Fireclay Boat	45 mins	1/3 filled		50 (Approx.)	1-2	5	Good crystals
13	650	100	Old Fireclay Boat	50 mins	1/2 filled		500 (Approx.)	.5-1.5	10	Good crystals but many spoiled by welding together
14	650	100	Old Fireclay Boat	50 mins	1/2 filled		500 (Approx.)	.5-1	10	As in 13
15	640	+	Old Fireclay Boat	50 mins	1/3 filled	Varied pressure; 3 mins at 100 cc/min. 1 min at 25 cc/min.	100 (Approx.)	.5-.75	10	Surface highly reflecting

TABLE I (cont.)

Boat Number	CONDITIONS OF GROWTH						RESULTS OF GROWTH			Comment
	Temperature (°C)	Flow Rate (cc/min.)	Substrate	Time	Amount	Other	Quantity	Average Length (cm)	Average Diameter (μ)	
16	650	100	→	50 mins	1/3 filled	Metal Boat	5	.3-.5	5	Fine crystals
17	650	100	→	50 mins	1/2 filled	1/2 reused boat mechanically cleaned; 1/2 chemically cleaned	nil			
18	650	100	→	50 mins	1/2 filled	As in 17	nil			
19	650	100	→	50 mins	1/2 filled	As in 17 but recharged halves	nil			
20	650	100	→	50 mins	1/2 filled	As in 19	nil			
21	650	100	Old Fireclay Boat	50 mins	1/2 filled		100 (Approx.)	.8-1.5	15	Good crystals

A whisker which was accidentally deformed is shown in Figure 17, showing slip lines propagating in two directions.

As noted in the introduction, the equilibrium cross-sectional shape of a small crystal should be the one of minimum surface free energy. For isotropic material this would conform to a circle, but for metals, where the surface free energy varies with orientation, the "equilibrium cross-sectional" shape is given by the Wulff Construction.

The cross-sectional shapes of some as-grown copper whiskers are shown in Figure 18. From this figure it is seen that the cross-sectional profiles are hexagonal, rectangular and square.

Attempts at identifying the orientation of the lateral faces proved unsuccessful. A conventional x-ray unit with a copper tube operating at 30 KV and 20 MA for twelve hours, did not produce any diffraction pattern. This was a consequence of the low intensity per unit area of the beam. Identifying the lateral faces by using an electron probe beam to produce a Kossel Line pattern was also unfruitful. Lack of information on exposure times and specimen to film distance, coupled with the difficult condition of the whisker moving in the electron beam, prohibited a Kossel pattern being obtained.

The method of identifying orientations using etch pit shapes was tried using dilute ferric-chloride solution. The resultant etch pits were diffuse and so ambiguous.

In the light of the above attempts it is not possible in this thesis to give a conclusive statement regarding the orientation of the lateral faces.

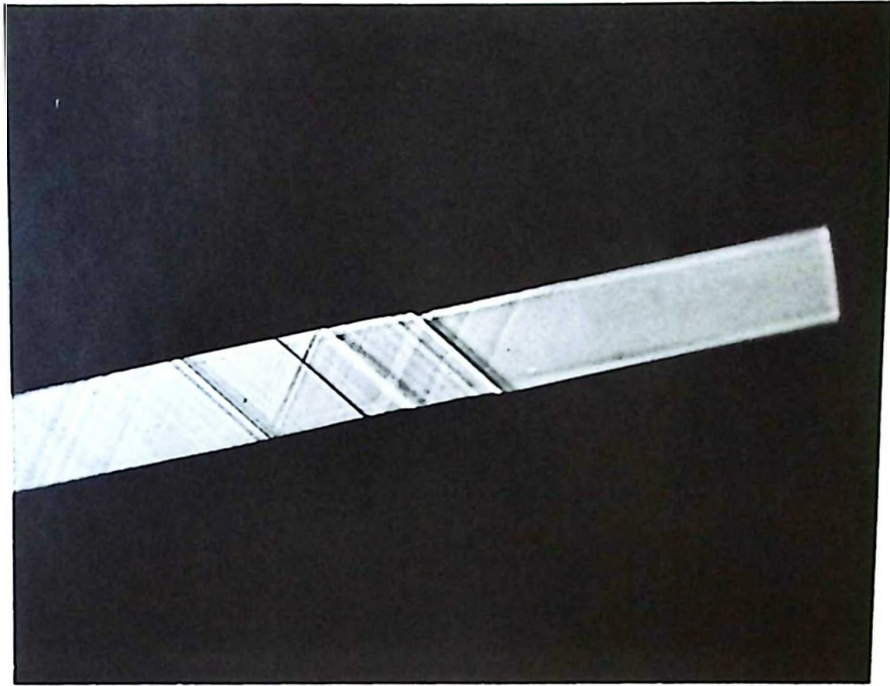


FIG. 17

DEFORMED WHISKER SHOWING SLIP LINES

PROPAGATING IN TWO DIRECTIONS

500 X
Before Reduction
For Publication

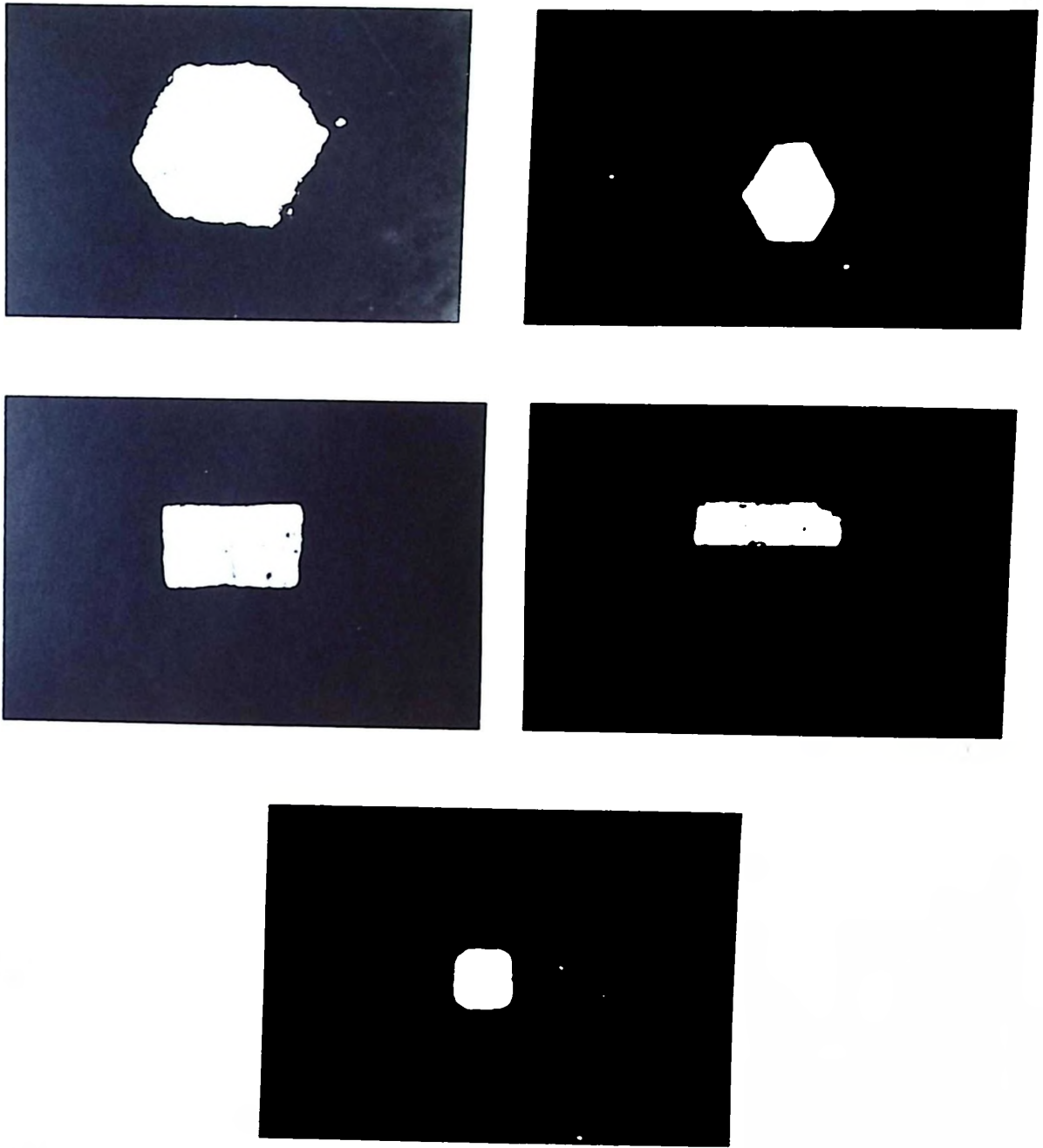


FIG. 18

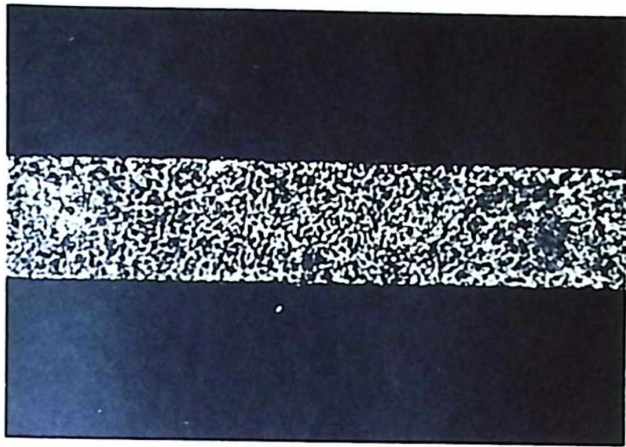
VARIOUS WHISKER CROSS-SECTIONS SHOWING TYPICAL
HEXAGONAL, RECTANGULAR AND SQUARE PROFILES

2000 X
Before Reduction
For Publication

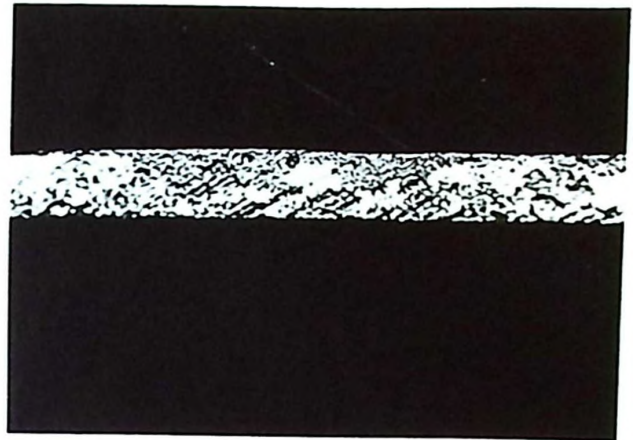
However, for a six sided figure whose growth axis is $\langle 110 \rangle$, a standard stereogram shows that the external faces may be $\{110\}$ or $\{112\}$. Mackenzie et al⁵⁵, using a broken bond model, have shown that the $\{110\}$ orientation has a relatively lower surface energy than the $\{112\}$ surface. Hence, it is suggested that the external faces are predominantly of the $\{110\}$ type.

Dissolution

To demonstrate that the system was at chemical equilibrium and that there were no changes in surface topography resulting from exchange currents, a whisker was immersed in the electrolyte for ten minutes. After this time it was re-examined using a 45x objective lens and no structural changes were observed. It was therefore concluded that, from the standpoint of surface topography, the system was in a state of equilibrium.



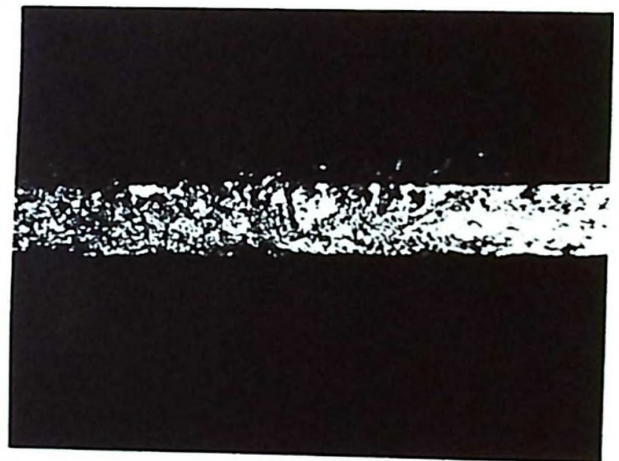
(a)



(b)



(c)



(d)

FIG. 19

CHANGE IN SURFACE TOPOGRAPHY OF WHISKERS ETCHED AT VARIOUS

CURRENT DENSITIES

2000 X
Before Reduction
For Publication

(a) Boat No. 4, 4
Current Density = 10 amps/sq. cm.
Time = 480 seconds

(b) Boat No. 4, 3
Current Density = 6.2 amps/sq. cm.
Time = 200 seconds

(c) Boat No. 4, 2
Current Density = 3.2 amps/sq. cm.
Time = 90 seconds

(d) Boat No. 4, 1
Current Density = 5.8 amps/sq. cm.
Time = 50 seconds

Crystals, selected from various boats, were employed as the anode of the electrochemical cell. The current density was gradually increased from zero over a range of 1 - 10 micro-amps/sq. cm. and the surface effects examined. Times were chosen so that the product of current density and time was the same for all cases. The topographical effects are illustrated in Figure 19.

Cross Sectional Results

A total of nine complete step-wise dissolution experiments were performed on the electrochemical dissolution of copper whiskers in copper sulphate electrolyte. Typical successive dissolution profiles of hexagonal, rectangular, and square whiskers are illustrated in Figures 20, 21 and 22, respectively and the corresponding width measurements in graphs 20A, 21A and 22A.

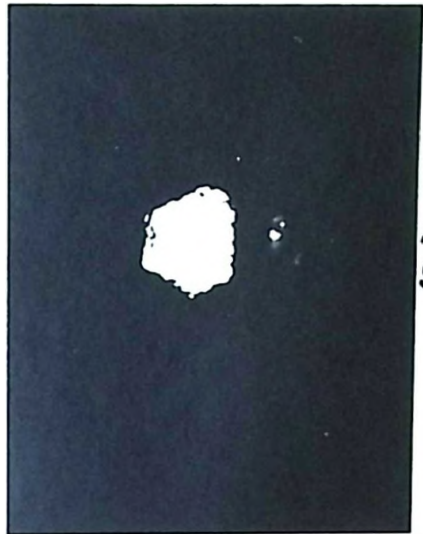
To ensure that the width difference actually refers to one orientation, the plots on any one graph are aligned so that their minima co-inside. No attempt is made to align the maxima positions, since these can change due to rapid dissolution of corners, especially with elongated whiskers. However, a crystal which dissolves maintaining its facets will also maintain its minima.

Graphs of the above type were established for nine dissolved whiskers and the average amount dissolved tabulated in Table II.

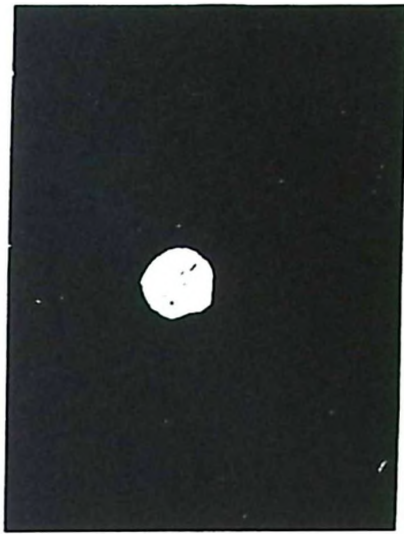
Division by the etching time yields the etching rate for a particular orientation. Since all the crystals were dissolved at different current densities, all the etching rates were normalized to a base of 1.5 micro-amps per square cm. for comparison purposes.

The average dissolution rate obtained by statistical treatment of the data is tabulated in Table III, for the major orientations of $\{110\}$, $\{112\}$, $\{123\}$ and $\{100\}$. The reciprocal of these values results in the reluctance rates or reciprocal dissolution rates.

The tabulated etch rates for the $\{110\}$, $\{112\}$ and $\{001\}$ planes are graphically represented in Figure 23, with the intermediate orientations of the $\langle 110 \rangle$ zone being interpolated.



(a)



(b)



(c)



(d)

FIG. 20

CRYSTAL 1,

POINT NO. 14,

2000 X
Before Reduction
For Publication

- (1) AS Grown
- (2) Etched at Current Density of 7.5μ amps/sq. cm. for 1 min.
- (3) Etched at Current Density of 7.5μ amps/sq. cm. for 5 mins.
- (4) Etched at Current Density of 7.5μ amps/sq. cm. for 9 mins.

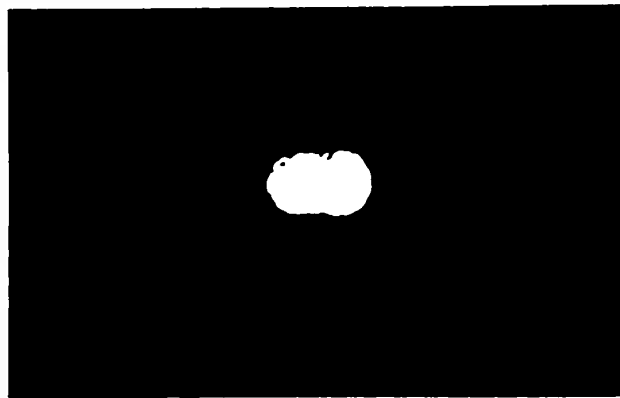
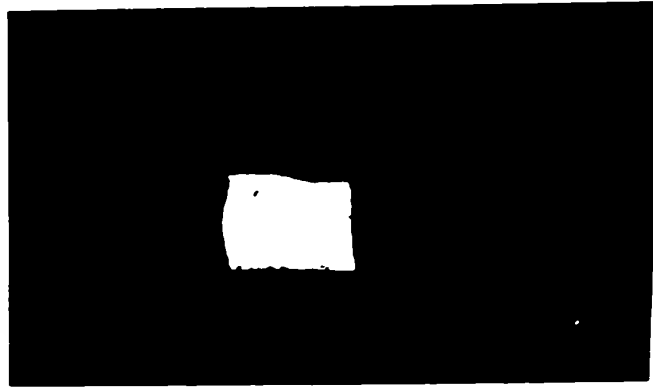


FIG. 21

CRYSTAL 4,

BOAT NO. 13

2000 X
Before Reduction
For Publication

- (1) As Grown
- (2) Etched at Current Density of 1.5μ amps/sq. cm. for 3 mins.
- (3) Etched at Current Density of 1.5μ amps/sq. cm. for 7 mins.

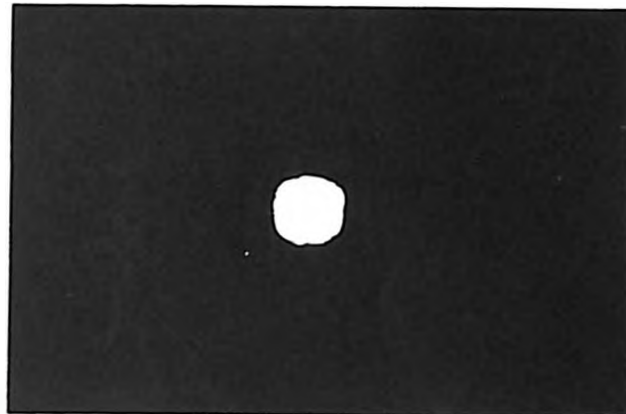
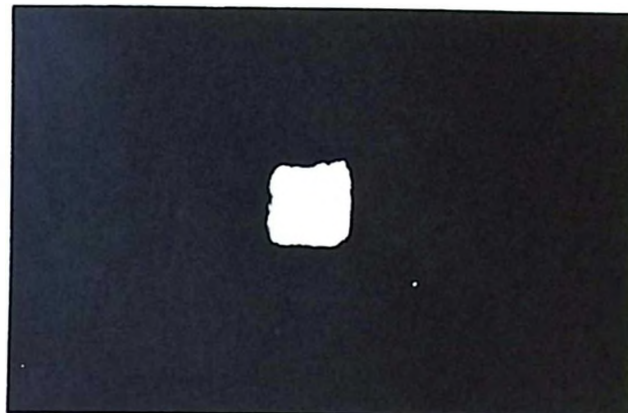
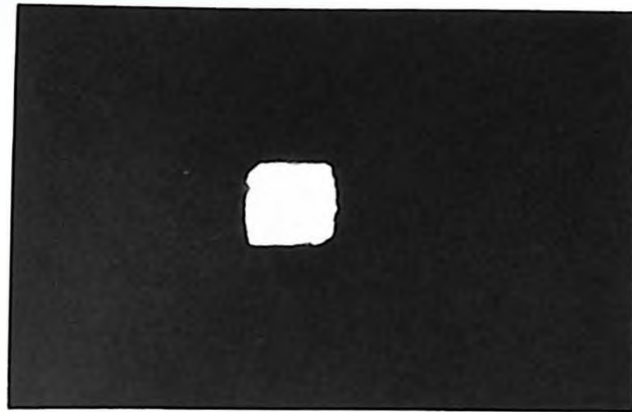


FIG. 22

CRYSTAL 8,

BOAT NO. 12,

2000 X
Before Reduction
For Publication

- (1) As Grown
- (2) Etched at Current Density of 8.2μ amps/sq. cm. for 3 min.
- (3) Etched at Current Density of 8.2μ amps/sq. cm. for 6 min.

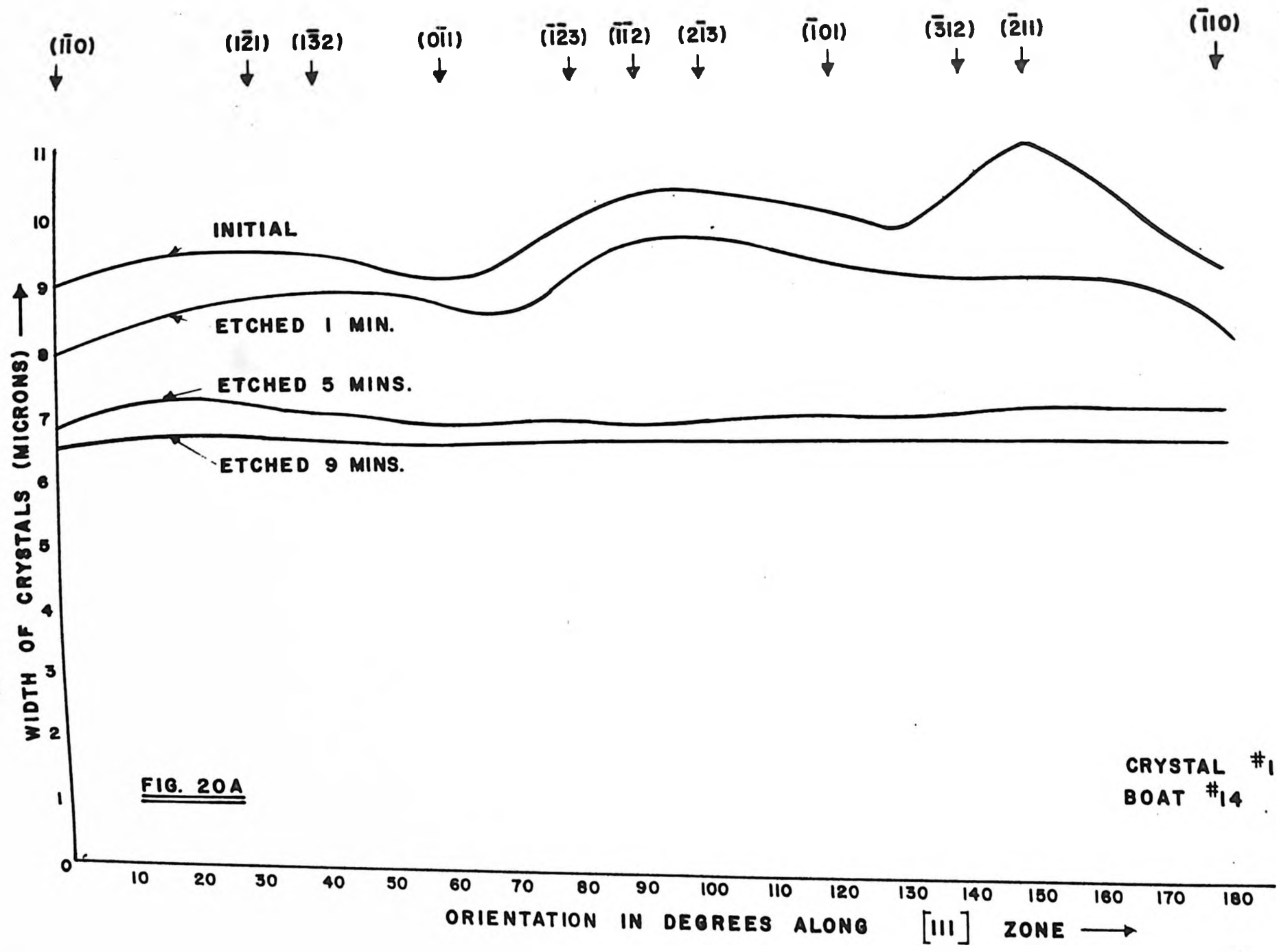
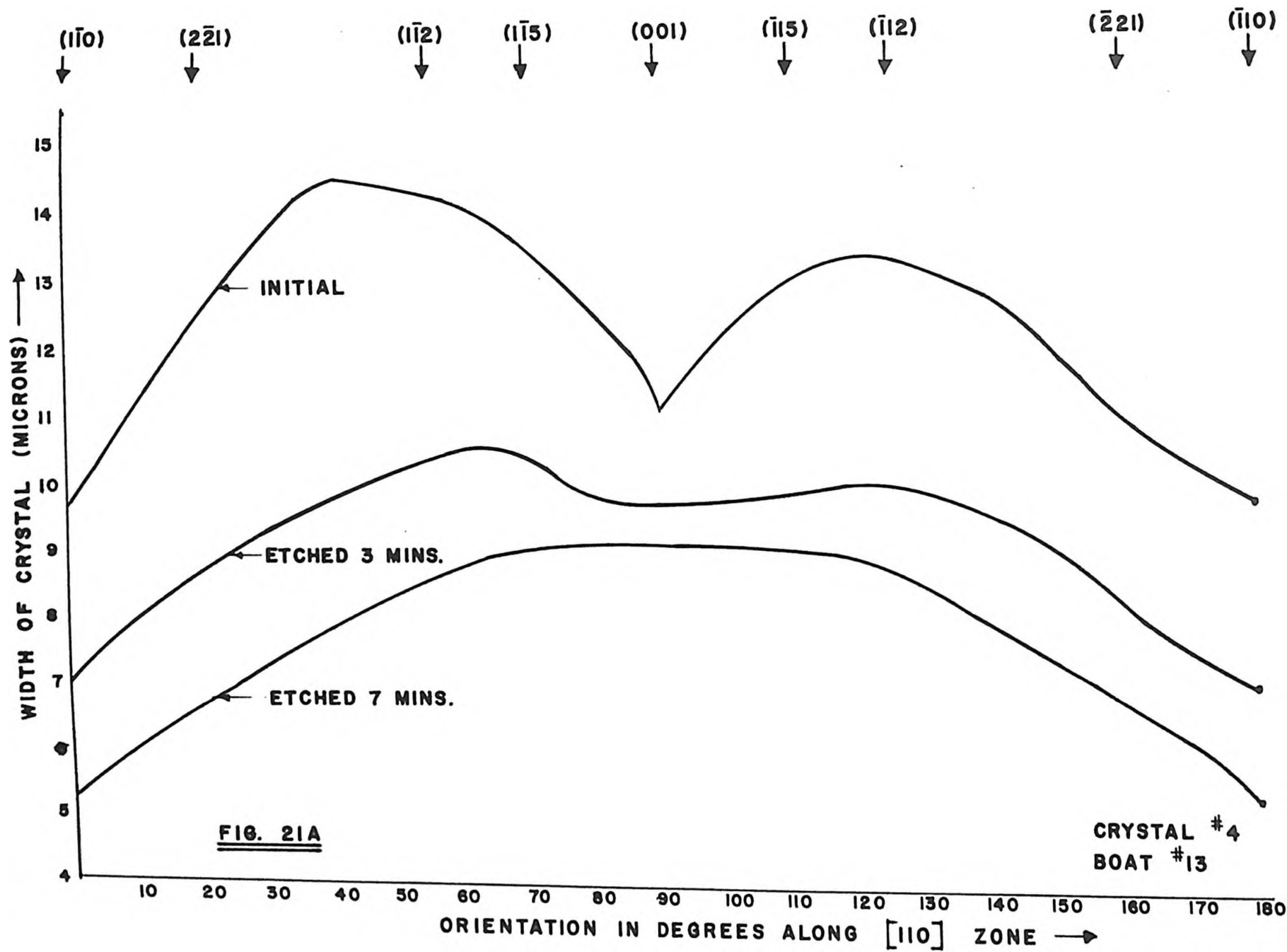


FIG. 20A

CRYSTAL #1
BOAT #14



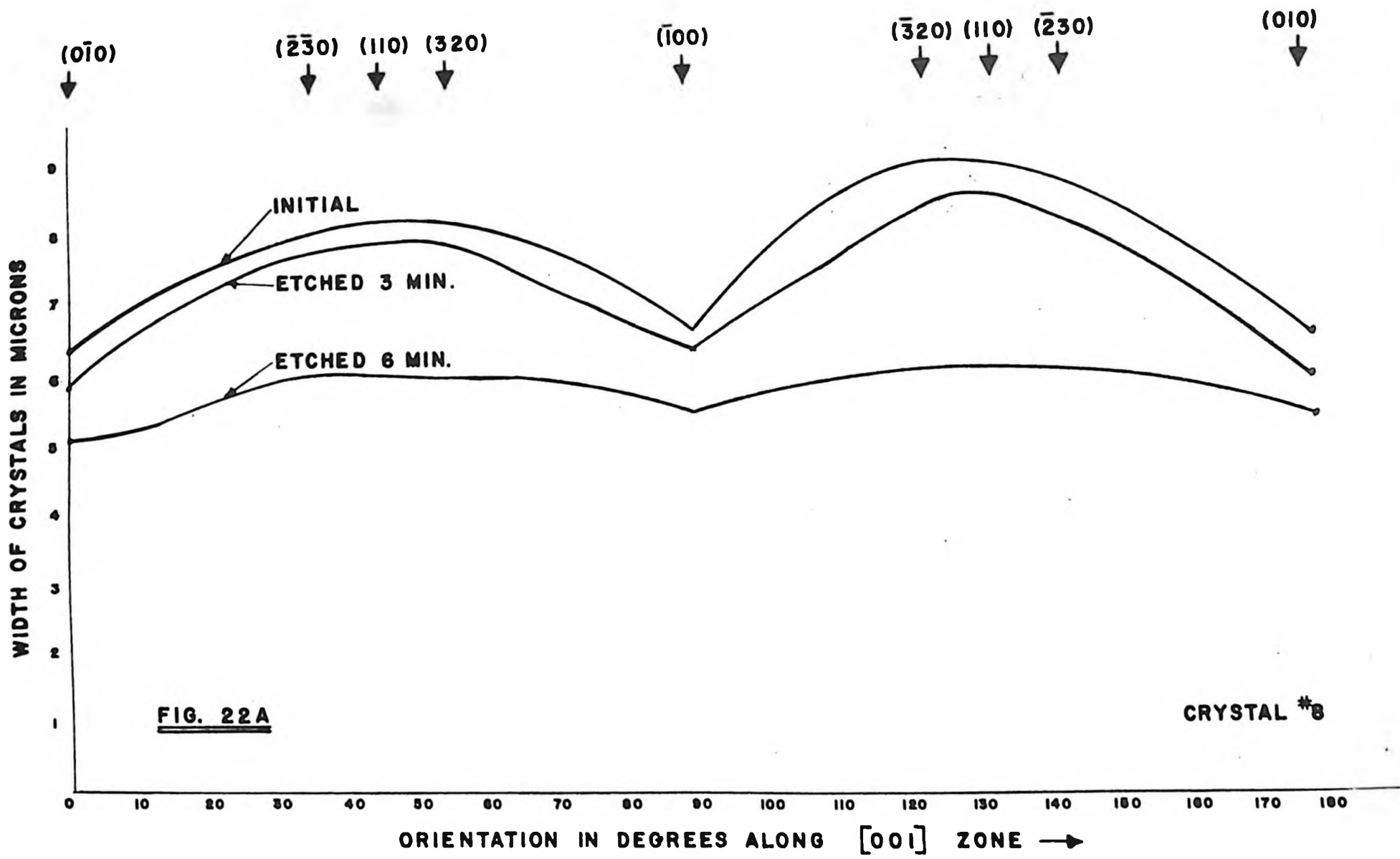


FIG. 22A

CRYSTAL #8

TABLE II
TABULATION OF DISSOLUTION DATA

Sample	Current Density (μ amps/sq cm) $\times 10^{-6}$	Time (mins)	Normalised Time (mins)	Orientation	Average Amount Dissolved (microns)	Etching Rate Normalised to 1.5 μ amps/cm ² (microns/min.)
No. 1	7.5	1	5	110	.67	.067
				112	1.13	.113
				123	.97	.097
		4	20	110	1.16	.029
				112	2.13	.053
				123	2.20	.055
		4	20	110	.25	.006
				112	.30	.007
				123	.20	.005
No. 2	2.45	3	4.9	110	1.40	.143
				112	1.63	.167
				123	1.90	.194
		3	4.9	110	.53	.054
				112	.80	.082
				123	.80	.082
		3	4.9	110	.625	.064
				112	.87	.089
				123	.95	.097
No. 3	1.0	8	5.34	110	.98	.092
				112	.90	.084
				123	1.15	.108

TABLE II (cont.)

TABULATION OF DISSOLUTION DATA

Sample	Current Density (μ amps/sq cm) $\times 10^{-6}$	Time (mins)	Normalised Time (mins)	Orientation	Average Amount Dissolved (microns)	Etching Rate Normalised to 1.5 μ amps/cm ² (microns/min.)		
No. 4	1.5	3	3	110	1.30	.216		
				221	2.90	.483		
				112	3.60	.600		
				115	3.10	.516		
				001	1.50	.260		
		4	4	4	110	1.80	.225	
					221	1.80	.225	
					112	1.60	.200	
					115	1.00	.125	
					001	.80	.075	
No. 5	2.6	5	8.66	112	2.20	.127		
				110	1.30	.075		
				123	2.20	.127		
No. 6	7.2	3	14.4	110	2.30	.079		
				112	2.76	.096		
				123	3.20	.112		
		3	14.4	3	110	1.95	.068	
					112	3.10	.106	
					123	3.80	.132	
		1	4.3	1	4.3	110	.40	.042
						112	.46	.047
						123	.42	.044

TABLE II (cont.)

TABULATION OF DISSOLUTION DATA

Sample	Current Density (μ amps/sq cm) $\times 10^{-6}$	Time (mins)	Normalised Time (mins)	Orientation	Average Amount Dissolved (microns)	Etching Rate Normalised to 1.5 μ amps/cm ² (microns/min.)
No. 7	9	3	18	110	3.90	.108
				112	6.36	.176
				123	6.40	.177
		3	18	110	.33	.009
				112	.36	.001
				123	.25	.007
		3	18	110	1.45	.040
				112	1.76	.049
				123	2.05	.057
No. 8	8.2	3	16.4	001	.26	.008
				110	.35	.016
		3	16.4	230	.475	.014
				001	.95	.029
				110	2.15	.065
				230	3.90	.119
No. 9	4	10	26.8	110	2.90	.054
				112	2.65	.049
				001	.70	.013

TABLE III

DISSOLUTION AND RECIPROCAL DISSOLUTION RATES

Orientation	Dissolution Rate Between Two Last Stages of Smooth Whisker				Average Dissolution (microns/min.)	(Average Dissolution Rate) ⁻¹ (mins/micron)
	No. 2	No. 6	No. 7	No. 8		
{110}	.064	.042	.040	.065	.053 ± .005	18.9
{112}	.089	.047	.049		.062 ± .018	16.1
{123}	.097	.044	.057		.066 ± .023	15.2
{001}				.029	.029	34.5

ETCH RATE OF COPPER WHISKERS IN COPPER SULPHATE ELECTROLYTE
AT CURRENT DENSITY OF 1.5 μ AMPS/SQ. CM.

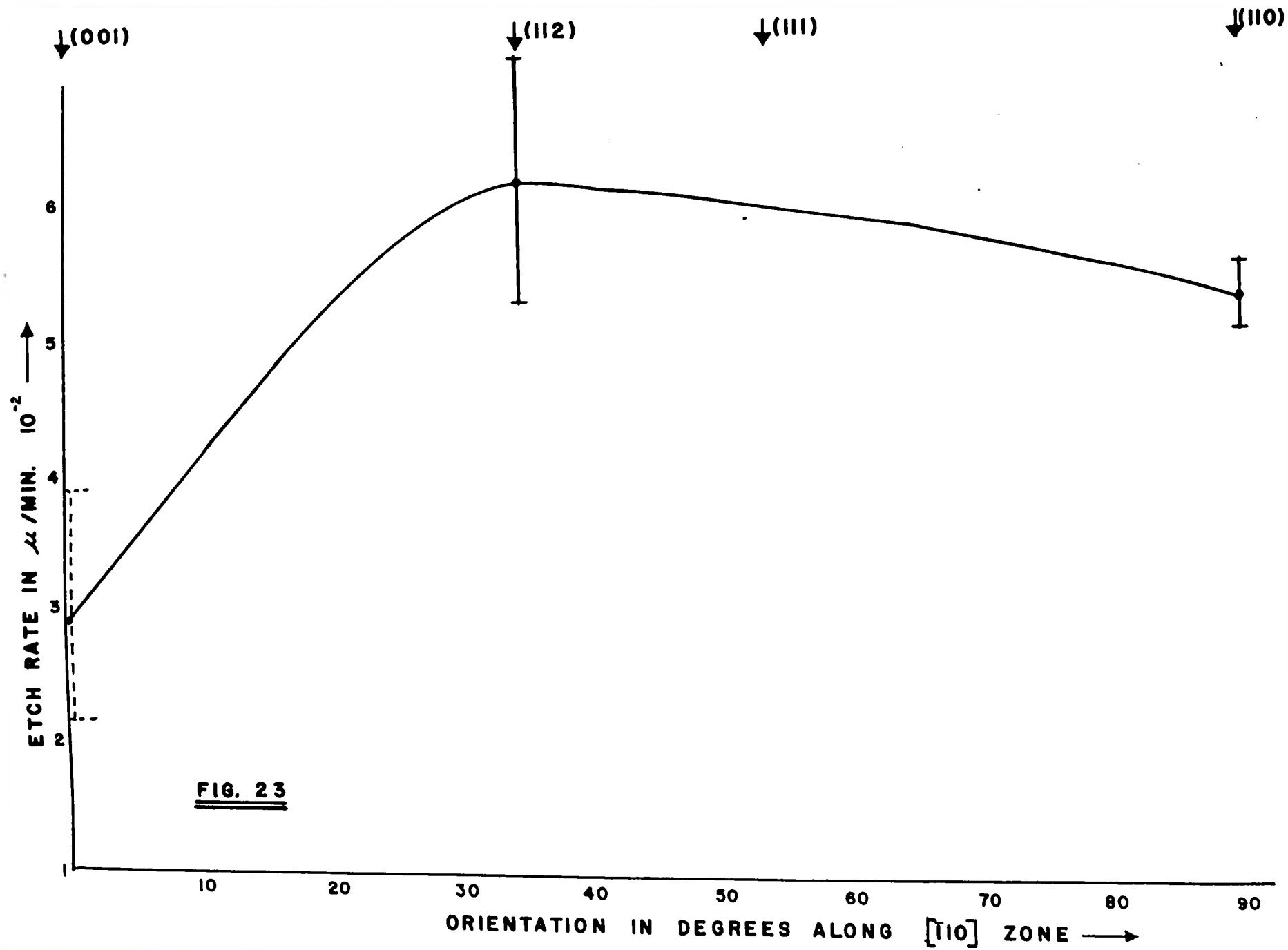


FIG. 23

CHAPTER VII

DISCUSSION

Introduction

Since the first reports in 1952 of the growth of metal whiskers displaying high strengths,⁴⁷ the operation of an axial screw dislocation in the growth mechanism has been attractive. This mechanism is based on the concept of a screw dislocation, emerging at the growth interface, providing a self-perpetuating step for the addition of new layers. Two-dimensional nucleation is unnecessary and growth can occur at a relatively small supersaturation. Lately, however, reservations have arisen regarding its universal application.⁴⁸ Axial screw dislocations have been reported for alumina, sometimes for palladium, but never in other metal whiskers. Subsequent work has confirmed these results.⁴⁹

Hirth⁵⁸ has considered the possibility of the whisker growing via an axial dislocation which then slips out of the crystal. This explanation for whiskers devoid of dislocations is only feasible when the diameter of the crystal is less than five microns.

Discussion of Growth Experiments

Examination of Table I shows that the growth of copper whiskers is inconsistent. From Table I it is seen that the temperature of the reaction is in the region of 650° c i.e. above the melting point of copper iodide (590° c). Basically the reaction for the production of copper whiskers is



This reaction could take place either homogeneously in the vapour phase, or, heterogeneously on the substrate or growing crystal. This question of a homogeneous versus a surface catalyzed reaction has been considered by Morelock and Sears,⁵⁰ who conclusively proved that the vapour phase from which copper whiskers grow by iodide reduction, is not highly supersaturated with respect to copper vapour. Hence, a homogeneous growth mechanism cannot be effective. This suggests that the carrier species through the vapour must be cuprous iodide and the reaction occurs on the whisker surface.

Thus from the information contained in Table I, three postulates may be made: (1) growth of copper whiskers occurs via the transport of cuprous iodide atoms which are (2) catalytically reduced by in situ impurities to copper and, (3) an axial screw dislocation is not essential for growth.

The activation analysis of copper whiskers gives a value of .01% iodine (Appendix II). This impurity content may explain the difficulties in attaining uniform dissolution of the whiskers. Consistent pitting resulted when the whiskers were dissolved. However, it was noted (Figures 20, 21, 22) that the pitting is most severe during the initial stages of dissolution and virtually disappears on further etching. The photographs in Figures 20-22 suggest that the impurities are concentrated on the surface of the whisker.

This finding is in agreement with Seastrom, Beck and Fontana.²³ These researchers, working on iron whiskers, found a very definite difference between the dislocation etch pits near the surface of the whisker and those near the centre. This led them to conclude that whiskers had two chemically distinct regions viz. the outside, or shell, and the core. The quantity and width of the shell etch pits were always the greater.

From the collection of these experimental results, a mechanism of the growth of copper whiskers by the reduction of copper iodide may be suggested, based upon the proposed theories of Webb,⁴⁹ Wagner et al.⁵¹ and Morelock and Sears.⁵⁰

Growth Mechanism

One might visualize the nucleation of whiskers as the nucleation of a liquid cuprous iodide droplet on the fireclay substrate. Impurities present, catalyse the reduction of cuprous iodide to copper and iodine, the catalysis taking place at the whisker tip. The remaining liquid becomes supersaturated with copper which precipitates, with a small concentration of iodine in solid solution. Continuation of this process causes the liquid alloy droplet to be displaced from the substrate resulting in whisker growth.

As was mentioned in Chapter III, the rapid growth rate necessitates the proposal of the carrier species being transported by surface diffusion along the whisker sides. Hence, one would expect a greater concentration of impurity on the whisker sides than in the bulk. This is indeed verified from many etching experiments (eg. Figures 20-22). An effect of the liquid cuprous iodide layer on the lateral surfaces seems to be one of growth inhibition, a necessary condition for whisker growth as postulated by Cabrera and Vermilyea.⁵²

Growth Morphologies

The cross-sectional shapes of Figure 18 represent the generally obtained whisker growth orientations. It is not necessary for the lateral faces of the whisker to expose the orientation corresponding to the smallest γ of the Wulff plot.

This has been substantiated from the work of Sunquist^{46,53} who showed that small (one micron) particles of copper, equilibrated in a hydrogen atmosphere at 350° C, adopted {110}, {111} and {100} faces. Similarly, Robertson and Shewmon⁵⁴ deduced a polar plot for copper in a hydrogen atmosphere which revealed only a 3% variation in the surface energies of {110}, {111} and {100}. A somewhat surprising feature of both these investigations is the good agreement between experiment and the predictions of a simple pairwise interaction model of surface free energy. This model, developed by Mackenzie et al⁵⁵ predicts a three dimensional polar diagram consisting of forty-eight spherical domes with all {100}, {110} and {111} planes corresponding to local minima.

On the other hand, Barns and Ellis⁵⁶ find that whiskers of gallium arsenide and gallium phosphate exhibit mainly {110} faces with a few {111}'s and {113}'s. However, it is possible that these higher index faces are the result of deformation during growth.

Dissolution

Due to the non-uniformity of the surface dissolution process, crystals from one boat -- boat 4 -- were selected and etched for comparison. The topographical effects are shown in Figure 19. These surface effects were obtained on different crystals such that the amount of material dissolved in each

case is approximately the same.

The successive dissolution profiles of a hexagonal, rectangular and square whisker are illustrated in Figures 20, 21 and 22 respectively. It is evident from these photographs that the cross-sectional profiles are by no means smooth. This roughness is undesirable since it prevents precise width measurements from being obtained. It is noted that the initial dissolved profile is always rougher than subsequent ones. This is thought to be an indication of greater impurity content at the surface resulting in preferential attack. Once the surface layers have been etched away, subsequent cross-sections are smoother, which substantiates the view that impurity concentration is greatest at the surface.

This fact that impurities in whiskers are in greatest concentration at the surface has been proven for iron whiskers by Seastrom et al.²³ The surface impurities represent a handicap when studying the dissolution of copper since they represent a deviation from the dissolution of intrinsic crystal.

The width measurements around the periphery of the three cross-sectional profiles of Figures 20-22 are plotted in Figures 20A, 21A and 22A. Now, in a $\langle 111 \rangle$ zone, rotation by 180 degrees passes through each plane at least three times. Hence, one obtains the width measurement of each orientation at three different places. Similarly, for a $\langle 110 \rangle$ zone, every orientation occurs twice upon rotation through 180°, as illustrated in Figure 21A, hence the calculated amount dissolved

is half the average difference in the width measurements obtained for the same orientation at two different places. Also, 180 degree rotation in a $\langle 001 \rangle$ zone passes through each orientation twice (Figure 22A) so that the amount dissolved is taken as half the average of both readings.

The average amount dissolved from the crystal faces obtained from graphs of the type 20A, 21A and 22A for all dissolved crystals is given in Table II.

Since the surface layers are not pure copper, to use the first etched profile to establish the etching rate of copper would introduce a statistical error. Hence, in obtaining the average dissolution rate of the copper whiskers, only the last two stages between smooth profiles have been taken into account. The average dissolution rate with its statistical deviation for principle orientations obtained from smooth etched profiles is given in Table III.

Unfortunately, the experimental error in measuring the dissolution rate of copper whiskers in this research was approximately 10%. Since there is only a 3% variation in the surface energies of the $\{110\}$, $\{111\}$ and $\{001\}$ orientations, then unambiguous detection of the whisker orientations by means of their etch rates is not possible.

From Fig. 23 it is seen that the dissolution rate (R) is in the order $R \{123\} > R \{112\} > R \{111\} > R \{110\} > R \{001\}$. However, the large overlap in the error bars of Fig. 23 means that this sequence could be in error. In fact, the

orientation dependence of the dissolution is quite ambiguous from the form of Fig. 23.

It should be noted that the above sequence of etching rates is in complete agreement with Robertson et al.⁵⁷ for the electrochemical dissolution of copper in aerated solutions of sulphuric acid. In the light of this fact, it is suggested that the dissolution rates are probably in the order $R \{123\} >$

$R \{112\} > R \{111\} > R \{110\} > R \{001\}$ but conclusive experimental evidence was not obtained in this research.

CHAPTER VIII

CONCLUSIONS

(1) The growth of copper whiskers was found to depend on the condition of the substrate and the condition of the furnace tube. Reused fireclay boats and an unclean silica tube were found to be necessary conditions for successful growth.

The necessary impurity was determined to be iodine which segregated to the surface.

(2) Growth probably occurs by copper produced from the reduction of copper iodide at the liquid tip.

(3) Unambiguous orientation dependence of the dissolution rates were not obtained owing to unavoidable experimental errors.

REFERENCES

1. Gibbs, J. W. "On the Equilibrium of Heterogeneous Substances." Longmans, Green and Co., New York, 1928.
2. Wulff, G. Z. Krist., 34, 449, 1901.
3. Frank, F. C. In "Growth and Perfection of Crystals." John Wiley and Sons, New York, 1953.
4. Cabrera, N. Diss. Faraday Society, 28, 16, 1959.
5. Kossel, W. Nach Ges Wiss Gottingen, 135, 1927.
6. Burton, J., Cabrera, N., and Frank, F. C. Phil. Trans. Royal Society, 243A, 209, 1951.
7. Herring, C. In "Structure and Properties of Solid Surfaces." Univ. of Chicago Press, 1955, p. 5.
8. Hirth, J. P., and Pound, G. M. J. Chem. Physics, 26, 1216, 1957.
9. Cabrera, N. In "The Art and Science of Growing Crystals." Edited by J. J. Gilman, New York, 1963.
10. Gordon, J. E., and Menter, J. W. "Mechanical Properties of Whiskers and Thin Films." Cambridge, 1958.
11. Pearson, Read and Feldman. Acta Met., 5, 181, 1957.
12. Cullity, D. B. In "Elements of X-Ray Diffraction." Addison-Wesley, 1956.
13. Hulett, L. D., Jr. Private Communication.
14. Young, F. W., Jr., and Hulett, L. P., Jr. In "Metal Surfaces." A. S. M., Cleveland, Ohio, 1963, p. 377.
15. Young, F. W., Jr., and Gwathmey, A.T. J. App. Physics, 31, 1960, p. 227.
16. Stossel, W. Acta Met., 9, 522, 1961.
17. Jenkins, L. H. J. Electrochemical Soc., 107, 371, 1960.
18. Bertocci, U. Inst. Lombardo. Rend. Sci., 91, 355, 1957.
19. Jenkins, L. H., and Stiegler, J. O. J. Electrochemical Soc., 109, 467, 1962.

20. Lovell, L. C., and Wernick, J. H. J. App. Physics, 30, 590, 1959.
21. Livingston, J. D. In "Direct Observations of Imperfections in Crystals." Interscience, New York, 1962, p. 115.
22. Shemanski, R. M., Beck, F. H., and Fontana, M. G. Corrosion, 21, 39, 1965.
23. Seastom, C. C., Beck, F. H., and Fontana, M. G. Corrosion, 19, 120t, 1963.
24. Frank, F. C. Diss. Faraday Soc., 5, 48, 1949.
25. Sears, G. W. Acta Met., 3, 36, 1955.
26. Gomer, R. J. Chem. Society, 38, 273, 1958.
27. Parker R. L., Anderson R. Harvey S. App. Phys. Letters, 2, No. 6, 1963.
28. Dittar, W., and Neuman, K. Z. Electrochem. Physik. Chem., 64, 297, 1960.
29. Lasko, W. R., and Tice, W. R. J. App. Physics, 33, 2045, 1965.
30. Drum, C. C., and Mitchell, J. W. App. Physics Letters, 4, No. 9, 1964.
31. Webb, W. W. In "Growth and Perfection of Crystals." John Wiley and Sons, New York, 1958, p. 230.
32. Wagner, R. S., and Ellis, W. C. App. Physics Letters, 4, 8, 1964.
33. Cabrera, N., and Levino, M. M. Phys. Rev., 96, 1155, 1954.
34. Lighthill, M. J., and Whitham, G. B. Proc. Royal Society, 81, 317, 1955.
35. Frank, F. C., and Ives, M. B. J. App. Physics, 31, 1996, 1960.
36. Ives, M. B. J. App. Physics, 32, 1554, 1961.
37. Ives, M. B., and Hirth, J. P. J. Chem. Physics, 33, 517, 1960.
38. Mullins, W. W., and Hirth, J. P. J. Physics and Chemistry of Solids, 24, 1402, 1963.
39. Chernov, A. A. Dokl. Akad. Nauk. SSSR, 117, 983, 1957.
40. Tagert, W., and Robertson, W. D. J. Electrochem. Soc., 102, 86, 1955.

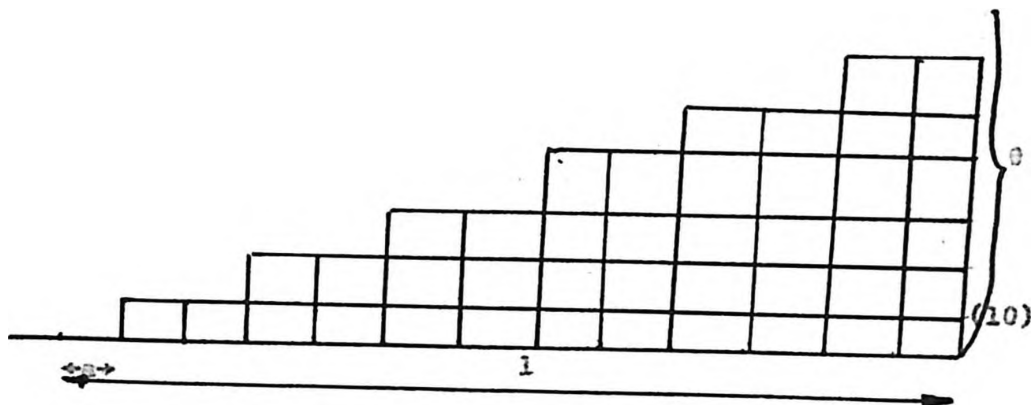
41. Chernov, A. A. Soc. Phys. Uspekhi, 4, 116, 1961.
42. Hulet, L., Jr., and Young, F. W., Jr. J. Chem. Phys. Solids, Aug. 2, 1965.
43. Brenner, S. S. Acta Met., 4, 62, 1956.
44. Saubestre, R. H. Ind. and Eng. Chem., 51, 287, 1959.
45. Brenner, S. S., and Morelock, C. R. Rev. Sci. Instruments, 28, 652, 1957.
46. Sundquist, B. Acta Met., 12, 97, 1964.
47. Doremus, Roberts and Turnbull. "Growth and Perfection of Crystals." John Wiley and Sons, New York, 1958.
48. Webb, W. W., Dragsdorf, R. D., and Forgeng, W. D. Phys. Rev., 108, 498, 1957.
49. Webb, W. W. J. App. Physics, 10, 214, 1965.
50. Morelock, C. R., and Sears, G. W. J. Chem. Physics, 31, 926, 1959.
51. Wagner, R. S., Ellis, W. C., Jackson, K. A., and Arnold, S. M. J. App. Physics, 35, 2993, 1964.
52. Cabrera, N., and Vermilyea, D. A. In "Growth and Perfection of Crystals." See Ref. 13, p. 393.
53. Sundquist, B. Acta Met., 12, 1964, p. 585.
54. Shewmon, P. G., and Robertson, W. M. In "Metal Surfaces." A.S.M., 1962.
55. Mackenzie, J. K., Moore, A. J. W., and Nicholas, J. F. J. Chem. Phys. Solids, 23, 185, 1962.
56. Barnes and Ellis, W. C. J. App. Physics, 36, July 1965, p. 2296.
57. Robertson, W. D., Mole, V. F., Davenport, W. H., and Talboon, F. P., Jr. J. Electrochem. Soc., 105, 569, 1958.
58. Hirth, J. P., Frank, F. C. Phil. Mag., 3, 1110, 1958.

APPENDIX I

Derivation of equation,

$$\gamma = \gamma_0 (\cos \theta + \sin \theta)$$

Consider a simple cubic structure with nearest neighbour bond approximation.



θ = angle from basal (10) axis

a = interatomic distance

Let $\gamma(\theta)$ = number of bonds on horizontal or vertical surface of orientation θ .

Let γ = number of bonds on horizontal or vertical surface.

Let ϕ = bond energy.

Number of bonds broken to form surface and mating surface

$$= \gamma(\theta)$$

$$= \left(\frac{1}{a} + \frac{1}{a} \tan \theta \right)$$

Now Surface Energy $\gamma = \frac{dW}{dA}$

$$= \frac{\phi \cdot \gamma(\theta)}{A} = \frac{\phi \left(\frac{1}{a} + \frac{1}{a} \tan \theta \right)}{2 \times \frac{1}{\cos \theta}} \quad (\text{where } A = \text{unit area of new surface created})$$

$$\gamma(\theta) = \frac{\phi}{2a} (1 + \tan \theta) \cos \theta = \gamma_0 (\cos \theta + \sin \theta)$$

$$\text{where } \gamma_0 = \frac{\phi}{2a}$$

This equation describes circles passing through the origin and having a diameter of γ_0 .

APPENDIX II

ACTIVATION ANALYSIS OF COPPER WHISKERS

9:40 t_c : 5 min 10 cm distance

99999	97451	16280	29135	18883	10826	10073	10428	11100	08896
07381	05587	06242	05804	05291	05292	05040	05063	04945	05120
05196	05212	05087	04932	04773	04650	04465	03939	03537	03179
02936	02731	02675	02543	02349	02326	02238	02178	02067	02314
02988	05665	11439	19134	25175	24745	17878	09940	04312	01880
01364	01691	02011	02122	01659	01080	00605	00366	00185	00155
00089	00104	00129	00106	00111	00061	00063	00055	00098	00039
00126	00170	00147	00171	00195	00144	00121	00059	00038	00062
00016	00051	00054	00040	00017	00033	00025	00041	00042	00047
00058	00080	00145	00167	00204	00237	00219	00295	00134	00095
00058	00051	00013	00008	00011	00017	99986	00010	00011	00009
00007	00017	00007	00015	99987	00002	00019	00003	99989	00002
99998	00004	00006	99986	00004	99985	99993	99999		

From the above results;

$$N = \frac{7.2 \times 10^6}{6.4 \times 10^{-24} \times 6 \times 10^{12} \times .56}$$

$$= 3.3 \times 10^{16} \text{ atoms iodine in .05 gm sample}$$

$$127 \text{ gms iodine} \equiv 6.02 \times 10^{23} \text{ atoms}$$

$$\therefore .05 \text{ gms iodine} \equiv 2.37 \times 10^{20} \text{ atoms}$$

$$\therefore \text{Average concentration of iodine in whisker sample}$$

$$= \frac{3.3 \times 10^{16}}{2.37 \times 10^{20}} \times 100$$

$$= 1.39 \times 10^{-2}$$

$$= .0139\%$$